



A review: The detection of cancer cells in histopathology based on machine vision



Wenbin He^a, Ting Liu^a, Yongjie Han^a, Wuyi Ming^{a,b,*}, Jinguang Du^a, Yinxia Liu^c, Yuan Yang^{d,**}, Leijie Wang^e, Zhiwen Jiang^a, Yongqiang Wang^f, Jie Yuan^a, Chen Cao^{a,b}

^a Henan Key Lab of Intelligent Manufacturing of Mechanical Equipment, Zhengzhou University of Light Industry, Zhengzhou, 450002, China

^b Guangdong HUST Industrial Technology Research Institute, Guangdong Provincial Key Laboratory of Digital Manufacturing Equipment, Dongguan, 523808, China

^c Laboratory Medicine of Dongguan Kanghua Hospital, Dongguan, 523808, China

^d Guangdong Provincial Hospital of Chinese Medicine, Guangzhou, 510120, China

^e School of Mechanical Engineering, Dongguan University of Technology Dongguan, 523808, China

^f Zhengzhou Coal Mining Machinery Group Co., Ltd, Zhengzhou, 450016, China

ARTICLE INFO

Keywords:

Machine vision
Traditional machine learning
Deep learning
Histopathological images
Cancer cell detection
Image preprocessing and segmentation
Feature extraction
Classification

ABSTRACT

Machine vision is being employed in defect detection, size measurement, pattern recognition, image fusion, target tracking and 3D reconstruction. Traditional cancer detection methods are dominated by manual detection, which wastes time and manpower, and heavily relies on the pathologists' skill and work experience. Therefore, these manual detection approaches are not convenient for the inheritance of domain knowledge, and are not suitable for the rapid development of medical care in the future. The emergence of machine vision can iteratively update and learn the domain knowledge of cancer cell pathology detection to achieve automated, high-precision, and consistent detection. Consequently, this paper reviews the use of machine vision to detect cancer cells in histopathology images, as well as the benefits and drawbacks of various detection approaches. First, we review the application of image preprocessing and image segmentation in histopathology for the detection of cancer cells, and compare the benefits and drawbacks of different algorithms. Secondly, for the characteristics of histopathological cancer cell images, the research progress of shape, color and texture features and other methods is mainly reviewed. Furthermore, for the classification methods of histopathological cancer cell images, the benefits and drawbacks of traditional machine vision approaches and deep learning methods are compared and analyzed. Finally, the above research is discussed and forecasted, with the expected future development tendency serving as a guide for future research.

1. Introduction

At present, cancer's dramatic rise in incidence and mortality has made it one of the world's top causes of death [1,2]. In the 2018 Cancer Survey, there were 18.1 million new cancer cases and 9.6 million cancer deaths. Lung cancer has the greatest fatality rate of any cancer on the planet, followed by colorectal cancer, stomach cancer, and liver cancer [3]. According to a recent cancer survey article, breast cancer has surpassed lung cancer as the leading cause of death worldwide, followed by lung, liver, stomach, and colon cancers [4]. One in eight women will develop breast cancer, a staggering prevalence [5]. The risk factors of

cancer (environment, food, age, etc.) are not easy to control, and the prevention and detection of cancer has become a hot topic [6]. Fig. 1 depicts the global number of new cancer cases and fatalities in 2020 for all cancer kinds. The World Health Organization's analysis and research concluded that if cancer patients are discovered in the early stages of the disease, the possibility of a successful cure can approach 80% [7]. Therefore, cancer detection is extremely crucial.

The methods of cancer diagnosis include clinical diagnosis, diagnostic medical imaging (DMI), surgical diagnosis, biochemical diagnosis and so on. Image diagnosis (X-ray, ultrasound, various contrast, nuclide, X-ray computed tomography (CT), magnetic resonance (MRI)) is the most commonly used diagnostic method by experts, while

* Corresponding author. Henan Key Lab of Intelligent Manufacturing of Mechanical Equipment, Zhengzhou University of Light Industry, Zhengzhou, 450002, China.

** Corresponding author.

E-mail addresses: mingwuyi@gmail.com (W. Ming), yangyuan@gzucm.edu.cn (Y. Yang).

Nomenclature

ACD	Adaptive color deconvolution
AP	All pixel
CDD	Charge-coupled Device
CNN	Convolutional neural network
DCAN	Deep contour-aware network
DDTNet	Dense dual task network
DRDA-Net	Dense residual dual-shuffle attention network
EGC	Early gastric cancer
FCM	Fuzzy c-means
FRST	Fast radial symmetry transform
GAN	Generative adversarial network
GLCM	Gray-level co-occurrence matrix
GVF	Gradient vector flow
HICN	Histological image color normalization
KM	K-means
LBGLCM	Local binary gray level co-occurrence matrix
LDED	Local double ellipse descriptors
MDE	Modified differential evolution
MST	Minimum spanning tree
NMF	Non-negative matrix factorization
PSNR	Peak signal to noise ratio
SCD	Specific color deconvolution
SPCN	Structure-preserving color normalization
SVD	Singular value decomposition
VB	Variational Bayesian

ACM	Active contour model
CapsNet	Capsule network
CM	Color map
DBLCNN	Dependency-based lightweight convolutional neural network
DCNN	Deep convolutional neural network
DNN	Deep neural network
DT	Decision tree
EM	Expectation-maximization
FCNN	Fully convolutional neural network
GAC	Geodesic active contour
GBM	Glioblastoma multiforme
GLRLM	Gray level run length matrix
HCC	Hepatocellular carcinoma
HIC-net	Histopathological image classification network
KNN	K-nearest neighbor
LBP	Local binary pattern
LFT	Local Fourier transform
ME-NBI	Magnifying endoscopy with narrow-band imaging
NCCN	New complete color normalization
PCA	Principal component analysis
SCAN	Stain color adaptive normalization
SFTA	Segmentation-based fractal texture analysis
SR	Sparse representation
SVM	Support vector machine
VT	Voronoi tessellation

histopathological image is the medical image obtained from biopsy tissue through microscope, so that experts can clearly observe the cell characteristic information in tissue [9,10]. For cancer diagnosis and grading, histopathological detection methods are considered the gold standard [11]. When the tissue is observed under the microscope, all structures show the same dark gray, so it is difficult to see the structural information and need to be dyed. In the histology lab, Hematoxylin and Eosin (H&E) staining is a commonly used staining procedure [12]. When chromatin in the nucleus and nucleic acid in the cytoplasm are stained with H&E, the components in the cytoplasm and extracellular matrix turn purple blue, while the chromatin in the nucleus and nucleic acid in the cytoplasm turn red, which enhances the information of tissue structure. Histopathological image has the advantage of free scaling, which can clearly show the micro details in the tissue image and improve the detection accuracy. Fig. 2 shows multiple magnification levels of the same histopathological image, from which the cellular structure information in the tissue can be clearly seen [13]. In traditional cancer testing, pathologists directly observe, analyze and grade these tissues through a microscope, which is a widely accepted standard for clinical cancer detection. However, pathologists are prone to dizziness and cervical fatigue under the microscope. Meanwhile, the pathologist

needs to take notes and write down the final decision, which is a time-consuming process [14]. With the rapidly increasing number of cancer patients, it is a time-consuming and laborious process for pathologists to manually analyze a large number of sections. In addition, manual diagnosis can lead to internal changes, inconsistencies and lack of traceability between observers. There is a 20% difference between experienced pathologists and novices in cancer diagnosis. A recent study showed that there was a 75.3% difference between individual diagnosis and expert diagnosis [15,16]. Therefore, a machine vision based detection approach is required. It has the ability to perform image quantitative analysis that is efficient, stable, and accurate. Machine vision technology overcomes the inconsistency between internal and external observers, in order to increase the precision and consistency of cancer detection and therapy.

Remote diagnosis and image analysis are advantages of machine vision technology, which overcomes the weaknesses of classical detection and enhances decision-making efficiency [17,18]. Compared with manual detection, machine vision technology is more efficient and objective, with higher precision. Traditional machine vision technology and deep learning vision technology have collided in recent years due to the rapid development of deep learning. For traditional machine vision

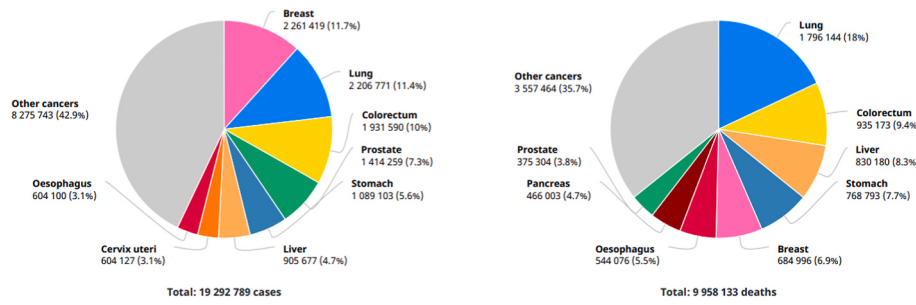


Fig. 1. New cases and deaths of all cancer types worldwide in 2020 [8].

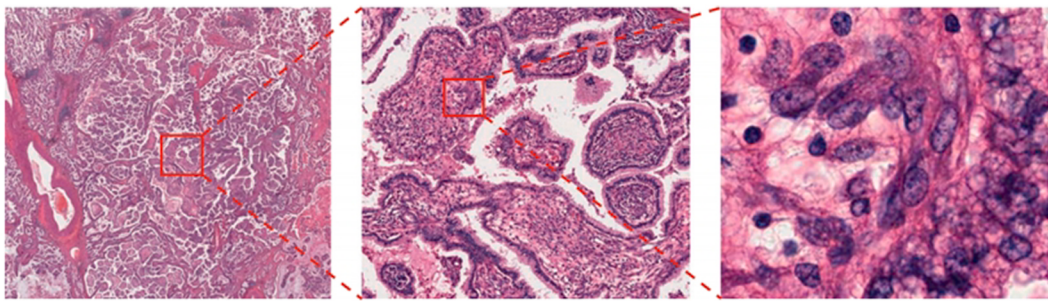


Fig. 2. Multiple magnification levels of the same histopathological image. Right images show the magnified region indicated by red box on the left images. Leftmost image clearly shows papillary structure, and rightmost image clearly shows nucleus of each cell. The histopathological images are adopted from TCGA [13].

detection technology, there are many excellent algorithms [19], but the data needs to be manually labeled, the operation is cumbersome, and the detection accuracy is relatively unstable [20]. As the number of classifications increases gradually, the classification and identification problems will become cumbersome or even difficult to achieve. Deep learning provides various advantages in recognition capabilities when compared to traditional machine vision technology [21]. It can obtain higher accuracy in image classification, semantic segmentation, target detection and other tasks. But deep learning relies on a large amount of labeled data [22] and is not suitable for general purposes. In addition, deep learning can be combined with traditional algorithms to overcome the challenges brought by deep learning in terms of computing power, time, characteristics, and input quality.

This study comprehensively summarizes the machine vision methods of cancer cell detection in histopathology, introducing machine vision methods for image preprocessing and segmentation, image feature extraction and image recognition, respectively. There have been many reviews on the use of machine vision to detect cancer in histopathology. For example, in the review published in 2009, Gurcan et al. [23] summarized the computer-aided design technology of digital histopathology, introduced the development and application of image analysis technology, and solved some specific histopathology related problems being studied in the United States and Europe. A review published by He et al. [11] in 2012 summarized the application of digital image processing technology in the field of histological image analysis. The latest image segmentation methods for feature extraction and disease classification were emphasized. In 2018, the review published by Komura et al. [24] described the use of machine learning techniques in the processing of digital pathological images, solved some specific problems and put forward possible solutions. In 2020, the review published by Das et al. [25] analyzed the application of various algorithms to breast cancer nuclei, discussed the challenges that need to be addressed, and outlined the importance of the dataset.

2. Background

2.1. Tumor grade, staging and classification

The grading of cancer is to observe the abnormal degree of cells in histopathology, that is, the growth and diffusion rate of tumor. The specialist will take a procedure called a biopsy to determine the grade of the cancer. Doctors remove some or all of the tumor tissue, cut the obtained tissue into really thin sections, usually with staining and other treatments, and look at the cell morphology and tissue structure under a microscope to determine whether the tumor is malignant or benign. At the same time, the pathological grade is also carried out according to the histopathological characteristics, that is, the grade of malignancy is determined [10,26]. Finally, experts formulate corresponding treatment plans by mastering the cancer grade, age and general health status of patients. At present, the grading and staging of tumor are important indicators for the diagnosis of tumor. In daily life, people generally

express the severity of tumors in early, middle and late stages. However, more accurate staging methods are often used clinically to describe tumor progression.

Tumor classification is a common classification task in clinical practice. Computer vision has described promising efforts, including most major cancer types, such as esophageal cancer, breast cancer, colorectal cancer, prostate cancer and so on. The pathological images corresponding to these cancers can distinguish the subtypes and grades of cancer through computer vision. Cancer grades and subtypes are related to different components or different degrees of canceration in the same tissues. Here, quantitative and qualitative analysis of cancer tissues are involved, which can be captured through deep learning. For example, computer analysis by deep learning model can distinguish normal tissue, atypical hyperplasia and adenocarcinoma in esophageal biopsy [27], invasive breast cancer, DCIS in situ, ductal carcinoma and benign tissue in breast cancer [28], and differentiate the subtypes of glandular polyp and polyp in colorectal cancer [29]. Gleason classification is the main classification scheme of prostate cancer. Computer vision has been developed to predict the Gleason classification of biopsy of prostatectomy specimens in clinic [30]. With the establishment of the proof of concept, and examples of cross-type cancer tissues continuing to show, demonstrating generalizability and practical value on computer vision will be the key challenge for detection and classification pathological image of cancer.

2.2. Image acquisition

In the 17th century, Leeuwenhoek invented a system for measuring microscopic objects, opening up the study of cells and tiny organisms [31]. After centuries of development, ultramicroscopy, phase contrast microscopy, fluorescence microscopy, electron microscopy, and scanning electron microscopy have emerged [23].

The detection of cancer by machine vision is mainly the recognition and classification of digital pathology images. Digital pathological images are high-resolution digital images that are scanned and collected using an automatic microscope or optical amplification device, and then automatically spliced and processed by a computer to produce high-quality visual data [32]. Before the emergence of pathological acquisition system, doctors examined histopathology or cytology under microscope, and their characteristic definitions often differed. Human visual perception and decision-making are dependent on a set of subjective, descriptive and intuitive norms that are difficult to replicate. The human visual system's complexity, processing speed and adaptability are also its flaws [14]. There are some deficiencies in the detailed interpretation of tissue sections directly observed by human eyes. Digital pathology overcomes the shortcomings of traditional methods. Compared with traditional pathology system, digital pathology system has the following advantages [33–36]: (1) Easy to store and manage. (2) Convenient browsing and transmission. (3) High speed, high efficiency and high throughput. (4) High resolution.

2.3. Computer aided diagnosis

Independent system identification and analysis are achievable with computer aided diagnosis, which may not be possible with human reviewing of an image alone. For example, molecular information can be predicted from standard H&E stained images, and immunohistochemistry (IHC) quantification can be done at the slide level [37,38]. Specific examples include identification of somatic mutations in lung cancer [39], estrogen receptor status in breast cancer [40], or consensus molecular subtypes in colorectal cancer from glass slides and stratified images [29]. In addition to computer analysis of pathological image, various deep learning computer techniques have also been created to improve cancer classification and subtype prediction. Many statistical and machine learning algorithms, such as microarray, RNA sequencing, quantitative polymerase chain reaction, NanoString, and tissue microarray, have recently been developed for the processing and interpretation of global molecular changes during the development and progression of cancer [41]. However, due to the difficulties of data acquisition, single-sample heterogeneity and high analysis cost, currently, traditional histopathological observation and assessment are used to stratify cancer patients.

2.4. Review structure

In parenchymal organs, a wide spectrum of diseases necessitate histological investigation, and cancer classification based on histological appearance and growth site is the most traditional diagnostic method in clinic. Unlike lung cancer, brain tumor and other tissues which diagnosed by CT or MRI, histopathological biopsy is highly targetable diagnostic method for solid cancer, such as breast, liver, gastrointestinal and pancreatic cancer. H&E or IHC stained slides provide microscopic views into tissue sections, allowing algorithms to exploit cellular and nuclear properties such as shape, size, color, and texture. According to the heterogenic character of cancer, obtaining and identifying marked biological information from sectional histopathological slides directly affect the clinical prediction, diagnosis and development of cancer diseases. Detection of histopathological images is the gold standard for the diagnosis of liver, breast and other cancers [42–45]. The histopathologic image contains sufficient characteristic information, which plays a vital role in the diagnosis and treatment of cancer. Therefore, this paper will focus on the computer visual and deep learning of the above pathological images of solid cancer.

As illustrated in Fig. 3, this study presents a complete evaluation of machine vision algorithms for cancer cell detection in histopathology. The first section discusses how machine vision can be used to detect cancer cells. The second section presents the clinical background of cancer cell detection. In section 3, we summarize, analyze and discuss machine vision methods for the preprocessing and segmentation of histopathology images. In section 4, we introduce shape, color, and texture feature extraction from histopathological images using traditional vision methods and deep learning methods. In section 5, we introduce traditional classifiers and deep learning classifiers to classify cancer cells and compare their accuracy. In section 6, we discuss the problems of traditional machine vision algorithms and deep learning algorithms for cancer cell detection. In section 7, we propose some potential issues and future research directions for machine vision methods for histopathological image detection.

3. Image preprocessing and segmentation

3.1. Image preprocessing

Image preprocessing is the processing that occurs before feature extraction, segmentation, and matching of input images in image analysis. The primary goal of histopathological image preprocessing is to remove unnecessary information from images, restore useful genuine

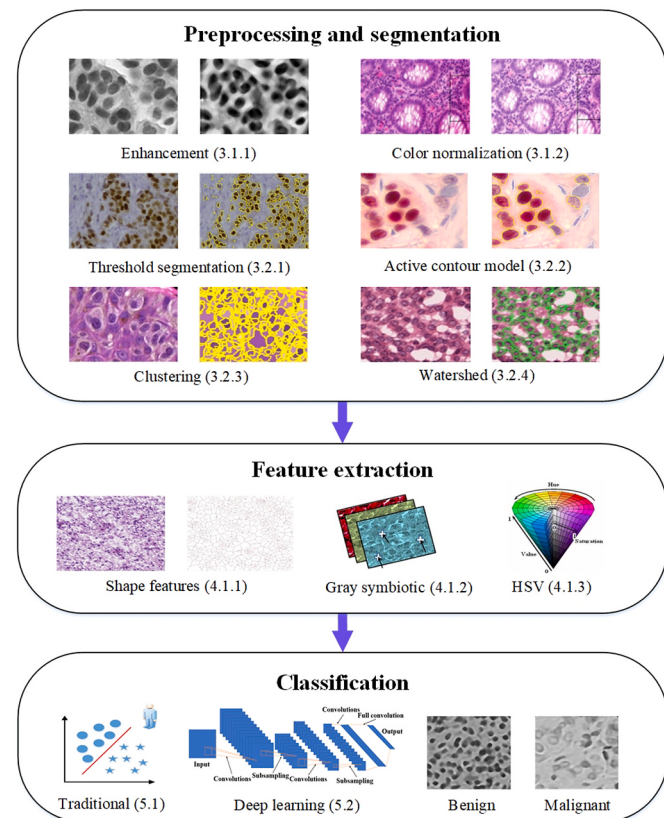


Fig. 3. Machine vision detection system for the detection of cancer cells in histopathology.

information, and improve the detectability of relevant information, which mostly entails image enhancement and color normalization.

3.1.1. Image enhancement

Image enhancement is the process of adding information or transforming data to an original image, selectively highlighting areas of interest in the image, or suppressing (masking) undesired features in the image in order to match the image with the visual response features. Frequency domain approaches and spatial domain methods are the two types of image enhancement. Grayscale transformation, histogram equalization, and filtering algorithms are the most common histopathological image improvement procedures.

Sertel et al. [46] proposed smoothing inhomogeneous regions of neuroblastoma with anisotropic diffusion, which could preserve important edge information. Similarly, Faridi et al. [47] first stained the nucleus with connective tissue and cytoplasm with H&E for color separation, and then used anisotropic diffusion filter after color separation, so that the image noise could be smoothed and reduced without removing important parts of the image content. Öztürk et al. [48] used 2D median filter to eliminate H&E paint imbalance in histopathological images, and then used adaptive histogram equalization method to effectively enhance the image, as shown in Fig. 4. Others utilized median filter to preprocess the breast histopathological image, which could not only remove the noise, but also preserve the image edge [49]. Wiener filter could also remove noise in color space [50].

Gaussian filter could reduce noise and enhance image [12,51]. Vahadane et al. [52] removed high-frequency noise through Gaussian smoothing, and enhanced the image with morphological filtering. It enhanced the segmentation and poor dyeing of different nuclei, and further smoothed high-intensity background and low-intensity foreground. In order to eliminate the background of breast tissue image and improve the contrast of input image, some people used the gray

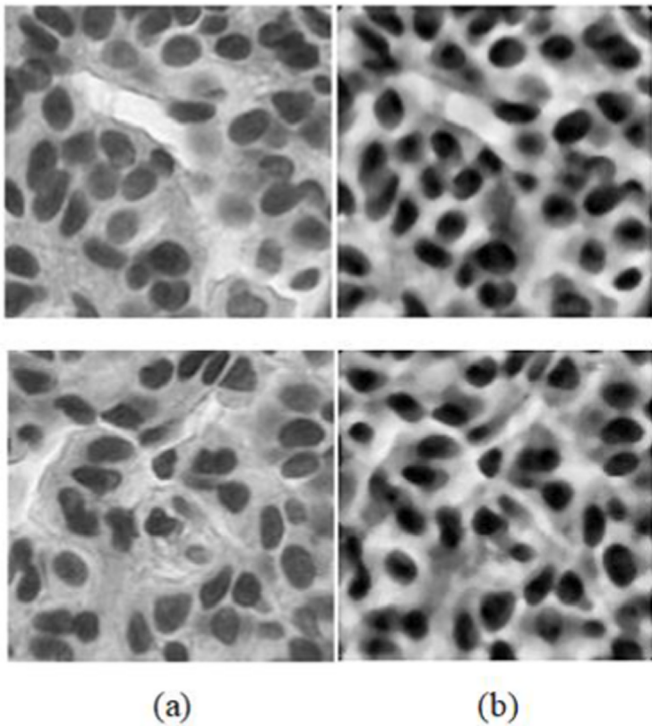


Fig. 4. Histopathological image enhancement [48]. (a) Original image. (b) After pre-processing method.

histogram equalization method to enhance the visual effect of the image [53,54]. López et al. [55] first recognized the nuclear contour through active shape models techniques, detected the cytoplasmic contour through parametric snakes, and used mathematical morphology techniques for image preprocessing. Some people also applied morphological method to eliminate the image threshold caused by noise [56]. Moreover, matched filters [57] and dynamic threshold segmentation method [58] can also enhance the image. The matched filter has a higher ability to smooth noise and maintain visual outlines than the typical Gaussian flat filter. Dynamic threshold segmentation is insensitive to illumination changes and has strong stability.

Table 1 summarizes the application of image enhancement technologies in histopathology. The spatial filtering process is simple, with a quick calculation time and a noticeable sharpening impact. The frequency domain filtering process is complicated and slow to calculate. It does, however, have the advantage of displaying the image effect reasonably smoothly. Gaussian, Wiener, and matched filtering are linear filters that are easy to implement. But linear filtering cannot remove salt and pepper noise. Median filtering and anisotropic filtering are nonlinear filtering, which can protect edge information, but are time-consuming.

3.1.2. Color normalization

In pathological cancer cell testing, tissue is sectioned and a sample for its staining is prepared. In general, the appearance of tissue staining varies depending on the staining ratio, the staining platform, and the imaging platform. However, due to the differentiated colors, the accuracy of image preprocessing and its quantitative analysis ability are affected. To address the above issues, the need for normalization of unwanted color changes in histopathology images is required [58].

Reinhard et al. [59] and Sertel et al. [46] both used histogramnormalizing method, which could remove unwanted color deviations in images. The non-negative matrix factorization (NMF) method proposed by Rabinovich et al. [60] and the singular value decomposition (SVD) method adopted by Macenko et al. [61] could normalize the

Table 1
Histopathological image enhancement.

Methods	Authors, year	Objective	Comments
Anisotropic diffusion (nonlinear)	Faridi et al. (2016) [47], Sertel et al. (2009) [46]	Neuroblastoma	Retain important edge information and reduce noise.
Median filter (nonlinear)	Öztürk et al. (2018) [48], Logombal et al. (2015) [49]	Breast	Remove noise while preserving edges.
Wiener filter (linear)	Öztürk et al. (2018) [50]	Tissue	It is suitable for stationary random processes, but not for non-stationary random processes.
Gaussian filter (linear)	Kleczek et al. (2020) [12], Kowal et al. (2013) [51]	Skin Breast	It has a good inhibitory effect on the noise obeying normal distribution.
Gray histogram equalization	Aswathy et al. (2020) [53], Mouelhi et al. (2018) [54]	Breast	Increase gray contrast.
Morphology	Vahadane et al. (2014) [52], Mohammed et al. (2013) [56], López et al. (2013) [55]	Cervix, Prostate, Lymph	It can effectively eliminate noise and retain the original information of the image.
Dynamic threshold	Dundar et al. (2011) [58]	Breast	Remove low brightness pigment.
Matched filter (linear)	Kamel et al. (2010) [57]	Follicle	Good ability to smooth noise and maintain image contour.

images, which could improve the ability of tissue image analysis algorithm, but the stability was not really good. Some people adopted a specific color deconvolution (SCD) method [62] to eliminate picture artifacts and increase the consistency of quantitative tissue image analysis. Hoffman et al. [63] quantitatively compared the effects of five normalization algorithms, including two global color normalization methods—all pixel (AP) and color map (CM) and three stain color normalization methods—K-means (KM), expectation-maximization (EM), and variational Bayesian inference (VB) on color segmentation performance. In the global color normalization procedures, the experimental results revealed that CM performed better than AP. KM performed the best among the stain color normalizing procedures. In general, stain color normalization approaches outperformed global color normalization approaches, so the performance of KM was better than or equal to CM. Dyeing color normalization utilizing KM clustering, in particular, demonstrated great dyeing segmentation accuracy and moderate computing complexity.

Some people proposed a new structure-preserving color normalization (SPCN) method [64]. Compared with other color normalization methods, this approach could split the source and target images, furthered the contrast of tissue image with inferior quality. Another method is histological image color normalization (HICN) considering biological characteristics and H&E characteristics [65], as shown in Fig. 5. This method was an improvement of the color normalization method of stained images studied by Vahadane et al. [64]. Among all normalization techniques, the average value of the perceived contrast measure of this method was the highest (36.14). Another new method was adaptive color deconvolution (ACD) [66], which had a high success rate of normalization and effectively solved the problems of structure and color artifacts. Stain color adaptive normalization (SCAN) method [67] could improve tissue-background contrast without affecting the backdrop color and preserving local areas. For H&E stained histopathology pictures, Vlijh et al. [68] suggested a novel complete color normalization (NCCN) approach, which improved the image quality, effectively solved the problem of inconsistent biopsy imaging and color variability, and had better variability compared with other benchmark

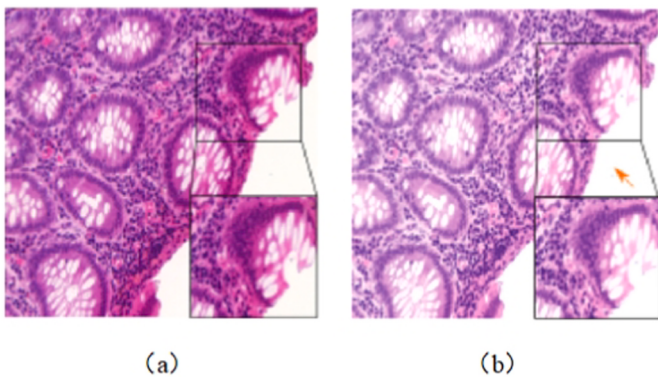


Fig. 5. HICN considering biological and H&E characteristics [65]. (a) Original image. (b) Color normalization results.

methods.

The above color normalizing methods are summarized in Table 2. Color normalization is an important aspect of pathological image preprocessing, and many color normalizing methods rely on dye density maps and color appearance estimation. Although color normalization can lessen chromatic aberration changes induced by staining and other factors, various changes in the tissue structure of the original image may occur during the procedure, affecting later image detection. Furthermore, it is necessary to explore the impact of color normalization

on following histopathological image detection tasks (image segmentation, feature extraction, and images classification) should be investigated.

3.1.3. Summary

Because histopathology images are more complicated than traditional images, they are contrast-enhanced in addition to being noise-free. Denoising and contrast enhancement are rarely used together in histopathology images. In instance, several researchers have successfully used threshold segmentation for denoising. Morphological filters have become popular in pathological picture improvement in recent years because to their versatility in corporate strategy.

3.2. Image segmentation

Image segmentation is a vital step between image processing and image analysis that involves splitting an image into multiple discrete sections with unique features and identifying objects of interest. Generally, the region of interest for pathological image segmentation mainly includes cell body, nucleus and cytoplasm outline. The commonly used histopathological image segmentation methods include threshold, active contour model (ACM), cluster, watershed segmentation and neural network.

3.2.1. Threshold segmentation

The threshold segmentation method, as shown in Fig. 6, is a region-based image segmentation technology, which divides image pixels into several categories. Its advantages are simple calculation, high operation efficiency and fast speed. Global threshold technique, adaptive threshold method, and local threshold method are the most extensively utilized histopathological tumor cell segmentation methods nowadays.

Gurcan et al. [70] suggested combining morphology and hysteresis threshold as a segmentation approach. This method was to segment the nucleus, and its average segmentation accuracy was as high as 90.24%, but its disadvantage was that it could not detect some faintly visible nuclei. Petushi et al. [71] used an adaptive threshold-based method for nuclear segmentation of breast histopathology images, which was also effective in identifying nuclei of nearly uniform pixel intensity. Lu and Mandal [72] put forward a local threshold method, which could effectively segment the complete nuclear region, as shown in Fig. 7. At the same time, this method retained the main components of the local circular region. Adaptive threshold segmentation method [73] and the Otsu threshold method [52] can be used for image segmentation. The result of adaptive threshold segmentation method was a better separation object, but this method had low discrimination ability for units with similar brightness. The Otsu threshold approach was the most common global threshold method because it avoided artifacts and improved histology image segmentation performance. The Otsu threshold approach, on the other hand, was unable to discern the fine and bright boundaries between cluster cores, resulting in enormous pseudo cores made up of numerous genuine cores. Based on increased morphology and an adaptable local threshold [54], all stained regions could be extracted and overlapped regions can be segmented.

Liu et al. [74] adopted a multi-threshold segmentation method based on modified differential evolution (MDE), which obtained 33 optimal peak signal to noise ratio (PSNR) evaluation mean values in terms of mean and variance. After a series of evaluation and analysis results, it could be seen that the segmentation method of multi-threshold segmentation method based on MDE could obtain better evaluation and analysis results. Kleczek et al. [12] proposed an approach based on a combination of statistical analysis, color threshold and binary morphology. The problem of front background segmentation of histopathological pictures of H&E stained skin specimens was efficiently solved using this method. Compared with other methods, this method was superior to similar methods with a Jaccard index of 0.929.

As can be seen from the previous literature review, threshold

Table 2
Color normalization method of histopathological images.

Methods	Authors, year	Advantages	Weaknesses
Histogram	Reinhard et al. (2001) [59], Sertel et al. (2009) [46]	Simple operation, balanced color distribution.	Large information loss.
NMF	Rabinovich et al. (2003) [60]	Decompose tissue samples stained with a variety of tissue dyes.	Dyeing leaks and co-localization cause errors.
SVD	Macenko et al. (2009) [61]	Improve the ability of tissue image analysis algorithm.	NThere is a negative value in the estimation of staining characterization.
KM	Hoffman et al. (2014) [63]	High dyeing segmentation accuracy, low computational complexity.	The performance is not extremely superior.
SCD	Khan et al. (2014) [62]	Reduce image artifacts, algorithm stability.	Poor preservation of structures and poor quality of the stain color.
SPCN	Vahadane et al. (2016) [64]	Separate the source image from the target image, improve the contrast of low-quality tissue learning image.	Perception pair is relatively small and complicated calculation.
HICN	Tosta et al. (2019) [65]	The average value of perceived contrast measure is the highest.	The high staining of tissue region has an influence on the estimation of W matrix.
ACD	Zheng et al. (2019) [66]	High success rate of standardization.	High computational complexity.
SCAN	Salvi et al. (2020) [67]	Improve the contrast between tissue and background without changing the background color and retaining local areas.	The input image size is too small, the separation may fail.
NCCN	Vijh et al. (2021) [68]	High image quality and good variability.	In the target image with high contrast, the synthesized image will be disturbed.

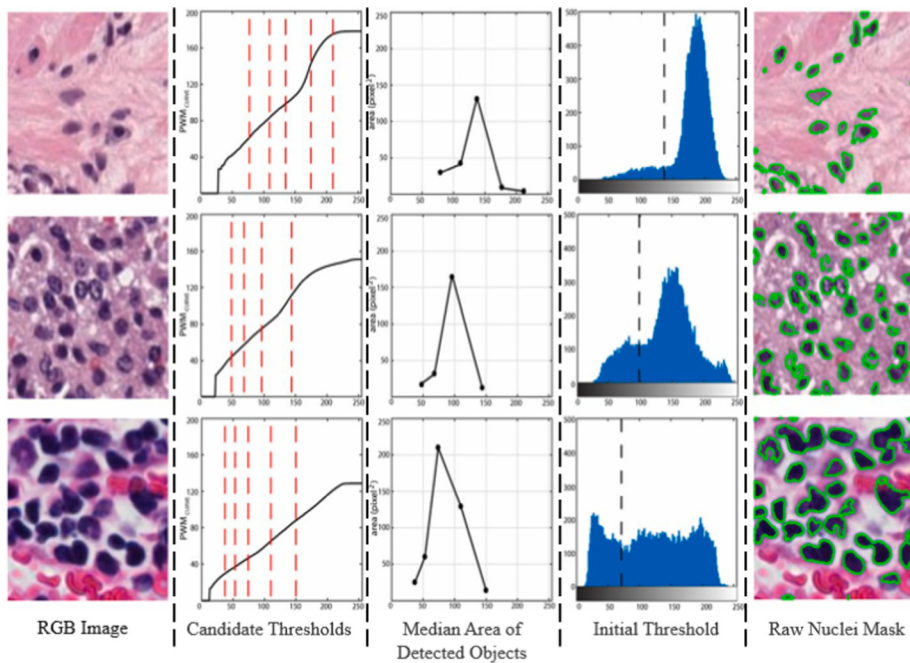


Fig. 6. Effectiveness diagram of histopathological image threshold segmentation method [69].

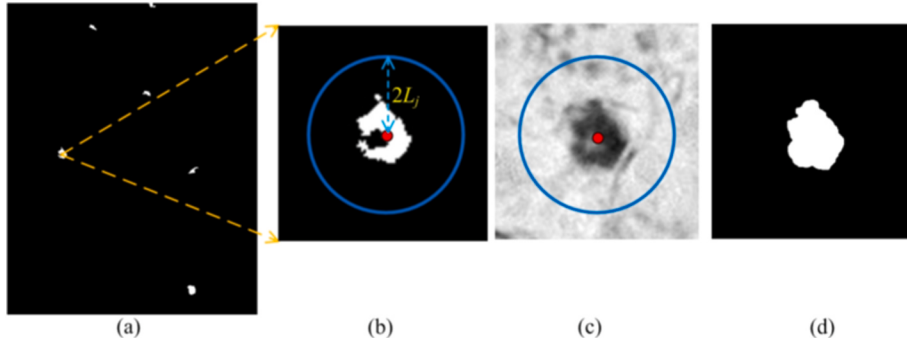


Fig. 7. Local threshold method [72]. (a) Several candidate mitotic cell regions. (b) A nonholonomic mitotic cell region. (c) Calculate the local threshold of this incomplete mitotic cell region. (d) The result of local thresholding in this mitotic cell region.

segmentation is appropriate when the contrast between the target and the background is high. The threshold segmentation approach is prone to over-segmentation and under-segmentation when the staining of histopathology images is uneven, resulting in segmentation failure. Several scholars have combined threshold segmentation with other segmentation to avoid over-segmentation and under-segmentation difficulties.

3.2.2. Active contour model (ACM) segmentation

The active contour model is an energy decreasing curve, which is dominated by the internal energy determined by the contour's own characteristics and the external energy determined by the image characteristics. It moves under the principle of minimum energy and finally stops near the edge of the object to be found. This model is one of the important tools for image segmentation and boundary extraction, mainly including gradient vector flow (GVF) model, snake model, geodesic model and so on.

For breast cancer cytology image segmentation, Malek et al. [75] developed a GVF snake approach. The form description accuracy of this method was higher than that of standard snake methods. Yang et al. [76] and Xu et al. [77] both adopted a color active contour model to divide the extracellular boundary. Fatakdawala et al. [78] used a method of

geodesic active contour (GAC) segmentation based on expectation maximization for the segmentation of lymphocytes in histopathological images of breast cancer. Experiments showed that the method had good robustness and accuracy.

Ali et al. [79] applied a new collaborative boundary and region ACM, which was used to segment the nucleus and gland structure of breast cancer. In addition, compared with other segmentation models, the model could solve the problem of 91% overlap in images. Mouelhi et al. [80] proposed an improved geodesic active contour model to extract the kernel boundary of each kind of image, the segmentation accuracy of the model was as high as 97%, which greatly improved the segmentation quality. For segmenting orphan annie-eye nuclei from histopathology pictures, Jothi et al. [81] employed a region-based active contour model, which could assist smooth rough boundaries and precisely capture the size and form of the nuclei.

To summarize, ACM has the ability to be computationally simple and handle the topological changes of curves during deformation. Its robustness in coping with sharp angles, topological changes, and initialization issues, however, is lacking. Gray edge gradients, for example, are prone to edge fractures and weak bounds in traditional ACM. The color gradient ACM has been improved to detect the proper cell edge, overcoming edge breakage and weak edge difficulties. The

GVF model has the advantage of being insensitive to initialization, being able to move into border pits, and accurately implementing picture segmentation.

3.2.3. Clustering segmentation

The core idea of clustering segmentation is that, in terms of the relationship between each pixel and adjacent pixels, if a pixel and adjacent pixels are highly similar in color, texture or grayscale, then they are merged into the same class. Clustering segmentation, which includes the K-means clustering method, mean shift clustering algorithm, and fuzzy c-means (FCM) clustering algorithm, is commonly employed in histopathology segmentation.

Sertel et al. [82] adopted K-means clustering algorithm with the number of clusters as four to distinguish the centroblast cells from noncentroblast cells. In addition, Sertel et al. [83] also used K-means clustering algorithm with the number of clusters as three to separate the cytoplasm from the nucleus. Dimitropoulos et al. [84] also applied K-means method to segment histopathological images. When segmenting some images with color variations, the K-means method was not suitable, so the mean shift [85] algorithm was needed. The mean-shift algorithm performed local clustering of pixels based on color similarity and spatial proximity, which could preserve local boundaries. Lu et al. [86] proposed mean-shift to segment the candidate kernel regions of the epidermal region, as shown in Fig. 8, the mean-shift segmentation method reduced the variation of local intensity while well preserving the boundaries of local objects. When there were only a few cores in the pre-segmented image, an improved segmentation method based on FCM needed to be used [87]. FCM, K-means, and ACM were compared by Aswathy et al. [53]. The K-means clustering approach, as shown in Fig. 9, was the most successful for segmenting cell nuclei.

To summarize, the most often used clustering algorithm is K-means clustering. The approach is quick and straightforward to use, however the number of clusters must be given, and choosing k is frequently difficult. The mean shift method, unlike K-means clustering, does not need the selection of the number of clusters, which is a benefit. The downside of the mean shift method is that the window size must be carefully chosen. FCM gives more flexible grouping results than K-means rigid clustering.

3.2.4. Watershed segmentation

The watershed segmentation algorithm is a mathematical morphological segmentation approach based on topology theory. It is a geographical morphology-based image segmentation technique that imitates geographical structures (such as mountains, ravines, and basins) to classify diverse objects. In the detection of nuclei in histology pictures, watershed segmentation is a computationally effective segmentation technique.

The nucleus of the images was segmented by Huang et al. [88] using a marker-controlled watershed transform and the GVF approach. This hybrid method was robust. George et al. [89] also adopted a marker controlled watershed transform to segment the nuclear boundaries in breast fine needle aspiration cytology images, which had high accuracy.

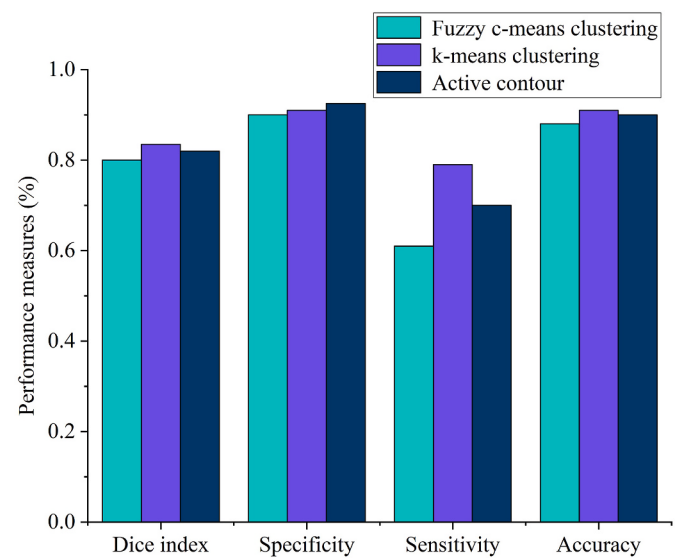


Fig. 9. Performance comparison of various clustering segmentation algorithms [53].

Jung et al. [90] proposed an H-minima transform-based watershed segmentation algorithm, which had a good segmentation effect. In order to identify the single cells, Dundar et al. [58] applied the watershed segmentation technique to segment the cell areas in breast cancer histopathology pictures in order to detect single cells. Veta et al. [91] used a multi-scale watershed segmentation method based on marker control to partition the H&E stained breast cancer histopathological images, and its marker enhancement and watershed segmentation process is shown in Fig. 10. Schüffler et al. [92] adopted a watershed-based cell segmentation method, which can accurately and high-throughput achieve cell segmentation. Mouelhi et al. [54] also applied this method to separate clustering or overlapping nuclei.

The watershed approach, on the other hand, makes it easy to excessively segment histopathological images. Some people produced a method that combined the watershed algorithm with Otsu optimal threshold [56]. By blocking the local minimum value of 1%, this approach avoided the problem of over segmentation and insufficient segmentation, and got the highest accuracy of 99.92%. However, it is vital to utilize controllable watershed indicators in order to limit lymphocyte loss. Moreover, Schmitt et al. [93] proposed a more effective grayscale based iterative voting method. To distinguish aggregation nuclei from fluorescence microscope cell pictures, Cheng et al. [94] employed the form marker and marker function in watershed method. The accuracy of this method was 6%–7% higher than that of the previous methods.

The fuzzy edge segmentation algorithm has a good segmentation effect on continuous edge contours. But it is extremely sensitive to disturbances in the image (noise and subtle grayscale differences) under

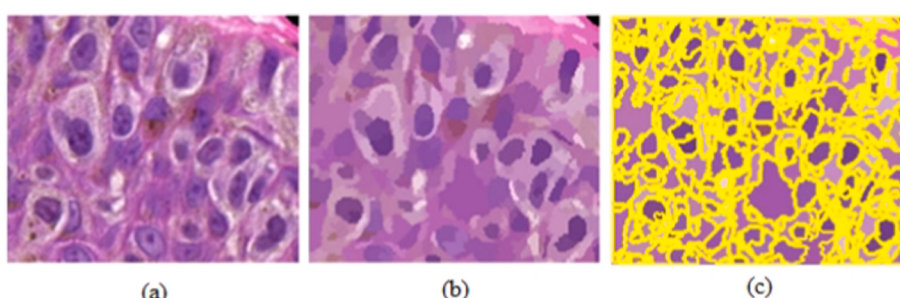


Fig. 8. Mean-shift segmentation [86]. (a) Original image. (b) Segmented image by mean-shift segmentation. (c) Boundaries of all the segmented regions.

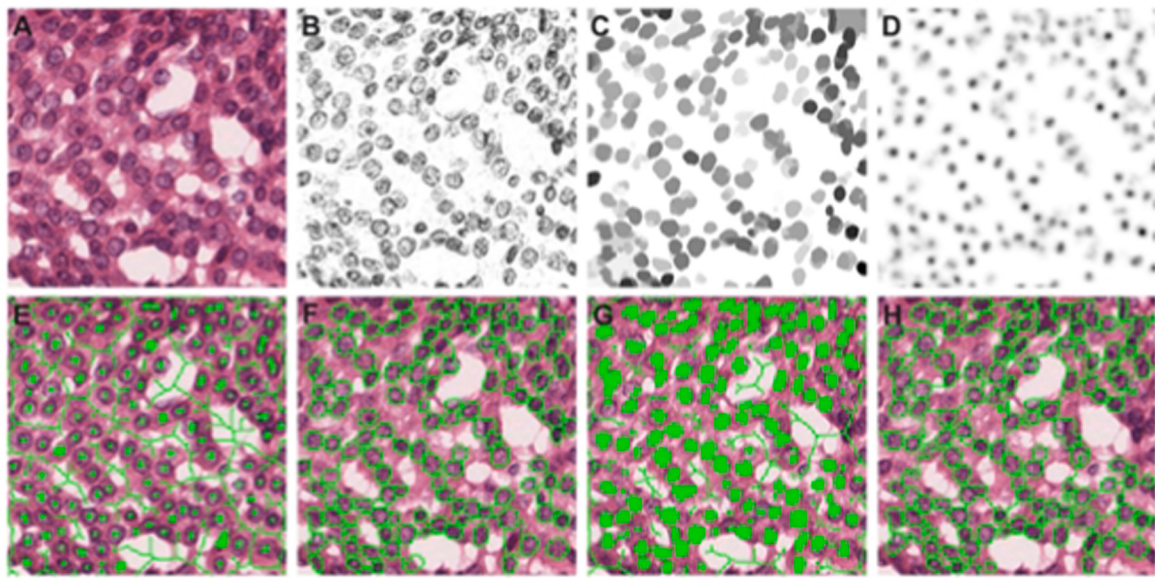


Fig. 10. Marker imposition and watershed segmentation for nuclei segmentation [91]. (A) Original image. (B) Hematoxylin channel. (C) Pre-processed image (hematoxylin channel processed with series of morphological operations). (D) Fast radial symmetry transform (FRST). (E) FRST foreground and background markers. (F) Watershed segmentation with FRST markers. (G) Regional minima foreground and background markers. (H) Watershed segmentation with regional minima markers.

which over-segmentation can easily occur. To solve the above problems, two methods are proposed to eliminate the over-segmentation phenomenon. One is to remove unnecessary edge information through observation processing; the other is to segment only the desired target through the improved gradient function. From the above literature review, it can be seen that the watershed algorithm is an effective image segmentation algorithm.

3.2.5. Neural network

At present, deep learning has been applied in many fields, among which neural network-based medical image segmentation methods have also sprung up. Wang et al. [95] proposed the detection of mitosis in breast histopathology images with convolutional neural networks. The technique can obtain reliable results rapidly without lots of computing resources and the accuracy could be further improved using a multi-layer convolutional neural network (CNN) model. Chen et al. [96] developed a unique deep contour-aware network (DCAN) that could detect and separate tissue objects in tissue images using a unified multi-task learning framework. The R2U-Net approach was utilized by Alom et al. [97] to segment nuclei. Experiments revealed that the approach was both resilient and accurate in segmentation (92.15%). Deep convolutional neural network (DCNN) [98] could perform semantic segmentation of various cell types in histopathology images with high segmentation accuracy. Fully convolutional neural network (FCNN) [99] could also be used for nuclear segmentation in histopathology images. Cui et al. [100] proposed an advanced supervised FCNN method for nuclear segmentation of histopathology images, which had high segmentation accuracy and fast segmentation speed. To segment nuclei, Kang et al. [101] adopted an approach based on the Unets network and deep layer aggregation. The method's generalization was demonstrated by the experimental results.

Torres et al. [102] suggested a DCNN-based approach for segmenting H&E-stained breast histopathology images, and the segmentation accuracy of this method was estimated to be 95.62%. Kucharski et al. [103] studied a convolutional autoencoder-based method for melanocyte segmentation, the sensitivity and specificity of this method were 0.76 and 0.94. This method proved that segmenting small ground truth databases was possible. Salvi et al. [104] proposed a gland segmentation method in prostate histopathology pictures that used deep networks

with standard techniques (CNN, ResNet-34, Unet). This approach received a 90.16% dice score. Zhang et al. [105] proposed a new type of dense dual task network (DDTNet), which could detect and segment tumor-infiltrating lymphocytes in histopathological images at the same time. Experiments showed that DDTNet had better detection and segmentation metrics compared to other advanced methods. Kiran et al. [106] employed the DenseRes-Unet model to segregate kernels in pictures, which was a deep, fully convolutional network. On multi organ nucleus segmentation, the model achieved an accuracy of 89.77%, which improved the segmentation of overlapping nuclei by 10%.

3.2.6. Summary

Table 3 displays a comparison of the histopathological cancer cell segmentation algorithms' overall performance. The segmentation accuracy of present picture segmentation methods is not perfect, as shown by the comparison study in **Table 3**, and has to be improved further. Threshold segmentation is the most often used picture segmentation algorithm, and choosing the right threshold is critical. Choosing the best threshold value can enhance segmentation accuracy significantly, but it takes time to do it. In the future, people's efforts will be concentrated on inventing high-speed segmentation algorithms.

Many studies have employed neural network methods to segment histopathology images, thanks to the rapid growth of deep learning. Using neural network for segmentation can improve the segmentation accuracy and is more suitable for the segmentation of histopathological images. But the deep learning algorithm's effect must be verified further because it is computationally costly and time-consuming.

4. Image feature extraction

Feature extraction is the transformation of raw features into a set of features with clear physical meaning (Gabor, geometric features, texture) or statistical significance. Feature extraction is related to dimensionality reduction because images are usually large and the subset of features to be computed is small [23]. The quality of the features has a crucial impact on the generalization ability. The primary study directions for pathological image feature extraction are shape, color, texture features and so on.

Table 3

Feature extraction method of histopathological image.

Types	Methods	Authors, year	Targets	Comments
Threshold	Morphology, hysteresis threshold	Gurcan et al. (2006) [70]	Neuroblastoma	High segmentation accuracy.
	Adaptive threshold	Petushi et al. (2006) [71]	Breast	Effectively identify nuclei with almost uniform pixel intensity.
	Local threshold	Lu et al. (2013) [72]	Mitos data set	It can segment the complete nuclear region.
	Adaptive threshold	Filipczuk et al. (2012) [73]	Breast	The result of separation is a better separation object, but it is difficult to distinguish units with similar brightness.
	Otsu threshold	Vahadane et al. (2014) [52]	Breast, Intestine, Prostate	It can avoid artifacts, but can not detect the fine and bright boundary between cluster nuclei.
	Adaptive local threshold, Morphology	Mouelhi et al. (2018) [54]	Breast	All stained nuclei can be extracted and overlapped nuclei can be segmented.
	Multi-threshold	Liu et al. (2021) [74]	Breast	Better evaluation results can be obtained.
	Color threshold, binary morphology	Kleczek et al. (2020) [12]	Skin	Stable results and segment blank spaces within tissue significantly better.
ACM	GVF-Snake	Malek et al. (2009) [75]	Breast	It is extremely effective in tracking the angle accuracy of cells.
	Color ACM	Yang et al. (2008) [76]	Lymph	It has high computational efficiency.
	Geodesic active contour	Fatakdawala et al. (2010) [78]	Lymph	It has good robustness and accuracy.
	A high-throughput ACM	Xu et al. (2011) [77]	Prostate	Fast and accurate segmentation of multiple objects in an image.
	A new collaborative boundary and region ACM	Ali et al. (2012) [79]	Breast, Prostate	It is able to better segment intersecting.
	An improved geodesic ACM	Mouelhi et al. (2013) [80]	Breast	Its segmentation accuracy is as high as 97%.
Clustering	A region based ACM	Jothi et al. (2016) [81]	Thyroid papilla	Smooth rough boundaries and accurately capture the size and shape of the nuclei.
	KM	Sertel et al. (2008) [82], Dimitropoulos et al. (2017) [84]	Lymph	Prior knowledge dependent on the number of clusters.
	Mean shift	Sertel et al. (2010) [85], Lu et al. (2013) [86]	Neuroblastoma, Skin	Local boundaries can be maintained.
Watershed	FCM	Filipczuk et al. (2011) [87]	Breast	Can better represent the nucleus.
	Improved watershed	Cheng et al. (2008) [94]	Mouse neuronal	Improve segmentation accuracy.
	Marker-controlled watershed transform	Huang et al. (2010) [88], George et al. (2013) [89]	Hepatocyte, Breast	Robust, high segmentation accuracy.
	Watershed segmentation based on H-minima transform	Jung et al. (2010) [90]	Breast	Good segmentation effect.
	Multi-scale watershed segmentation method	Veta et al. (2013) [91]	Breast	Effective kernel segmentation.
	Watershed, Otsu threshold	Mohammed et al. (2013) [56]	Lymph	The problem of over segmentation and insufficient segmentation is reduced, and the segmentation accuracy is high.
Neural network	Watershed segmentation algorithm	Dundar et al. (2011) [58], Schüffler et al. (2015) [92], Mouelhi et al. (2018) [54]	Breast	It can realize cell segmentation accurately and high throughput.
	CCN	Wang et al. (2014) [95]	Breast	Accurate results can be obtained quickly without a lot of computing resources.
	DCAN	Chen et al. (2017) [96]	Colorectal, Glioblastoma	It can accurately detect and segment tissue targets in tissue images.
	R2U-Net	Alom et al. (2018) [97]	The dataset	This method has good robustness and high segmentation accuracy.
	DCNN	Öztürk et al. (2019) [98], Torres et al. (2020) [102]	Breast	Semantic segmentation is carried out for various cell types, and the segmentation accuracy is really high.
	An advanced supervised FCNN	Cui et al. (2019) [100]	Breast	The segmentation accuracy is really high and the segmentation speed is fast.
	Unets, Deep Layer Aggregation	Kang et al. (2019) [101]	Bladder, Colorectal, etc	This method can be easily popularized in different cell types of different organs.
	Convolutional autoencoder-based	Kucharski et al. (2020) [103]	Melanocyte	It has high sensitivity and specificity.
	CNN, ResNet34, Unet	Salvi et al. (2021) [104]	Prostate	High dice score.
	DDTNet	Zhang et al. (2022) [105]	Breast	Better detection and segmentation indicators.
	DenseRes-Unet	Kiran et al. (2022) [106]	Breast, Stomach, Prostate, etc	High segmentation accuracy and good heavy core segmentation effect.

4.1. Traditional feature extraction

4.1.1. Shape features

Shape feature is a global or local feature used to describe the shape of an object. Common shape features can be divided into two categories, one is the contour feature that describes the shape of the boundary of the object. Because shape features are not dependent on the image's pixels, they are unaffected by changes in the image's grayscale and brightness.

Common shape features of histopathological images include geometric, moment and topological features.

The average distance between the centroids of the adjacent nuclei in high-density regions was derived as a feature for identifying histological images by Petushi et al. [71]. Lu et al. [86] used local double ellipse descriptors (LDED) to measure the local features of candidate regions, and to distinguish melanocytes from potential nuclear areas, researchers employed two LDED parameters: regional ellipticity and local pattern

characteristics. Experimental results showed that the method was more than 80% sensitive to segmentation of melanocytes. Tashk et al. [107] analyzed mitosis in histopathological images by extracting stiffness matrix, which included morphological, shape and geometric features. Wang et al. [108] suggested a new automatic feature-based analysis scheme for the classification of histopathology images that extracted form features, statistical features, and textual features. Fukuma et al. [109] extracted features from pathological images of brain tumors, including object-level features and spatial-arrangement features. The spatial-arrangement feature descriptors used included voronoi tessellation (VT), delaunay triangulation and minimum spanning tree (MST), as shown in Fig. 11.

Finally, the segmentation effect has an impact on the accuracy of shape feature extraction. Even shape characteristics cannot be derived from images with poor segmentation results. Cancer cells, for example, have uneven shapes, thus obtaining the shape of irregular items will yield misleading findings. There are now just a few studies on cancer cell shape extraction, and greater attention should be devoted in the future.

4.1.2. Color features

Color is the most commonly employed visual characteristic in image retrieval, owing to the fact that color is frequently associated with the object or scene depicted in the image. Furthermore, when compared to other visual qualities, color attributes are less sensitive to the image's size, orientation, and viewing angle, resulting in greater resilience. Color

features, on the other hand, are extremely sensitive to grayscale information and image brightness variations. Color normalization is required for the extraction of color features, considering that pathological images require staining.

Sertel et al. [110] suggested a color texture feature construction approach based on nonlinear color quantization. They combined the statistical features of mbrid construction with the hierarchical color and texture features of mbrid, which significantly improved the classification performance of the system, with an overall classification accuracy of 83.7%. Xu et al. [77] converted an RGB color image of prostate histopathology into the HSV color space using a color gradient function, removed the hue and saturation channels to generate a scalar luminance, grayscale image. Color gradient representations of digitized prostate histopathology images produced more pronounced borders relative to grayscale gradients. Kong et al. [111] utilized the new color space to obtain the color texture of each pixel point in histopathology pictures using the local Fourier transform (LFT). The color texture features extracted by this method had a good discrimination effect for classification. Some people [112] normalized the color distribution by aligning the 2D histograms of color distribution in a model based on hue, saturation, and density, and normalized it, and the stability of the normalized image was better. Rashmi et al. [113] used the RGB and LAB color spaces to extract the color properties of each pixel in order to observe the varied color distributions of nuclei and other tissue cells. The extracted color features improved the performance of the kernel

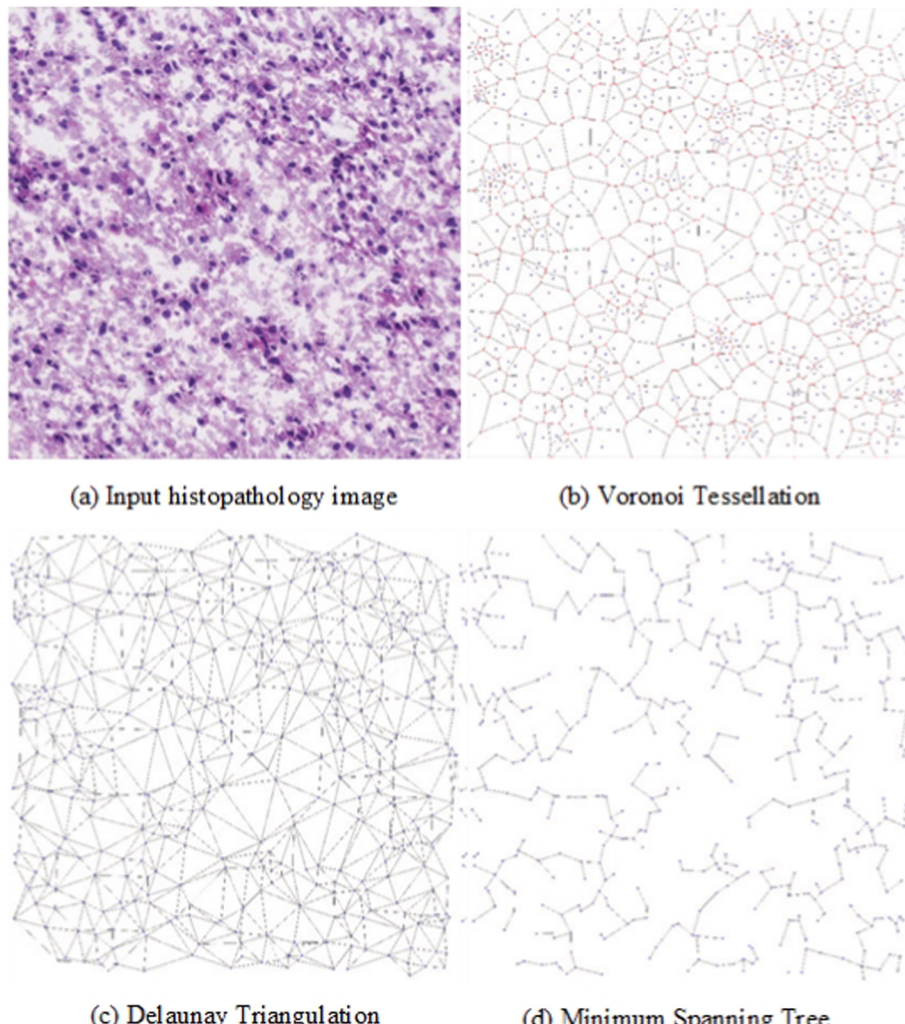


Fig. 11. Sample spatial arrangement feature extraction [109].

semantic segmentation algorithm. Chen et al. [114] used Python to extract and quantify the color features of magnifying endoscopy with narrow-band imaging (ME-NBI) images and gastric mucosal cancerous surface pathological images, as shown in Fig. 12. Gastric cancer lesions under ME-NBI had been studied to have a pink color change, which was a useful marker for the identification of early gastric cancer (EGC). Kumar et al. [115] applied color correlogram to extract the color distribution and spatial information of pixels in photographs. In this study, 1024 color features were extracted using this method, and it was observed that the morphology of cancer cells was mostly uneven in shape and color. There are no powerful discriminative features in a color correlogram because it uses only one color space. The author further extracted 33 color features using the color layout method, which could give information about the color distribution in the grid-like structure.

The variety of color models available gives us a lot of alternatives when it comes to extracting color characteristics. Because histopathological images are typically stained to create apparent color changes in cancer cells, the color properties of cancer cells are extremely important feature information. Color photographs contain more information than grayscale images, but processing color images is complex and time-consuming, hence grayscale images are commonly used.

4.1.3. Texture features

Texture is a visual quality of uniformity in an image that reflects the object's surface structure and organization qualities that change slowly or frequently. Texture features are used to describe the surface properties of the scene corresponding to the image or image area, such as the thickness and density of the image texture. It is a kind of global feature that's unaffected by color or brightness. Because it is immune to image rotation changes and noise, texture feature extraction is the most extensively used feature extraction approach.

Gray level co-occurrence matrix (GLCM) is a more effective and widely used approach for texture feature extraction. GLCM is a joint distribution that describes the gray level of two pixels with a certain spatial position relationship. As shown in Fig. 13, GLCM (1,1) has three groups in the original image, hence $p(1,1) = 3$, while GLCM (2,0) has only two groups in the original image, so $p(2,0) = 2$. Sertel et al. [83] proposed a new color-texture analysis method for computer grading of follicular lymphoma images, which was an improvement on the gray-scale co-occurrence matrix method and was suitable for the analysis of H&E stained pathology images. This method outperformed gray texture analysis and significantly improved classification performance. Albayrak et al. [116] used the Haralick texture feature descriptor method to extract features from breast cancer histopathology images, and then used GLCM as the input of the Haralick method. Krishnan et al. [117] applied Gabor filter to extract texture features from oral histopathology, and the extracted features were used for classification with 95.7% accuracy, 94.7% sensitivity and 98.8% specificity. Bruno et al. [118] adopted a curvelet transform, local binary mode (LBP), and statistical analysis-based feature selection approach. The LBP operator was performed on the curvelet transform coefficients of breast tissue images, and then the eigenvectors were obtained. The obtained ratio was in Between 91% and 100%.

2	1	1	0	0
1	2	1	1	2
0	0	1	2	0
2	2	0	2	1
1	2	1	1	0

0	2	1	1
1	3	3	4
2	2	4	1

Fig. 13. Gray-level co-occurrence matrix.

Phoulady et al. [119] used histogram of oriented gradients to extract texture information to classify cervical cancer and healthy cervical tissues. The accuracy rate was 93.33% and the false negative rate was zero. For automatic categorization of colorectal and prostate tumor biopsy samples, Peyret et al. [120] developed a new multispectral multiscale local binary pattern feature extraction method. The accuracy of the algorithm on different data sets was 99.6%. The GLCM method, the LBP feature extraction algorithm, the local binary gray level co-occurrence matrix (LBGLCM) feature extraction method based on the combination of the LBP algorithm and the GLCM algorithm, the gray level run length matrix (GLRLM), and the segmentation-based fractal texture analysis (SFTA) algorithm were investigated by ÖzTÜRK et al. [121]. The GLCM feature matrix generated in this study could successfully represent images with fewer parameters. The LBP algorithm was simple to calculate and resistant to grayscale changes. The LBGLCM method needed to consider all texture structure and spatial information when extracting features. GLRLM was a texture representing the model, using high-order statistics to extract the spatial plane features of each pixel, and SFTA was a good feature extraction method. After analysis, among all the classifier algorithms, the SFTA algorithm had the highest success rate (94.3%), and the LBP algorithm had the lowest success rate (84.2%). ÖzTÜRK et al. [50] compared the results of different feature extraction methods on cell detection to determine which algorithm was more successful. The features determined by these feature extraction algorithms are shown in Fig. 14 (a). The maximum stable extreme value region algorithm outperforms other algorithms in terms of detection, and it can identify numerous cells as well as mark the surrounding environment. Fig. 14 (b) depicts the performance of commonly used feature extraction algorithms.

Although the texture characteristics retrieved by GLCM have high identification capacity, they are detached from the human visual model and do not use global information. The LBP method is easy to compute and can be used to detect in real time, however it has limited capacity to represent features and lacks rotation invariance. Several researchers have combined the local information provided by LBP with additional information or approaches to build joint feature quantities to improve extraction results.

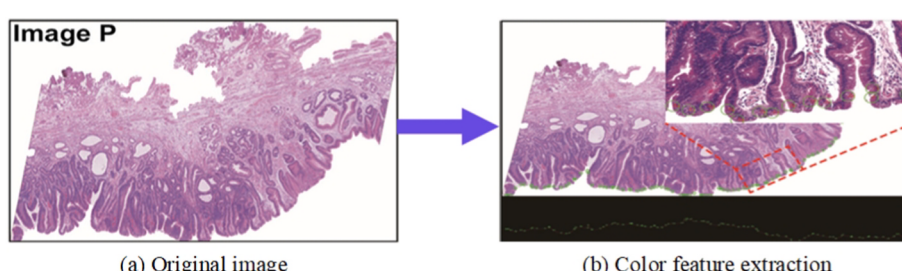


Fig. 12. Color feature extraction with Python [114].

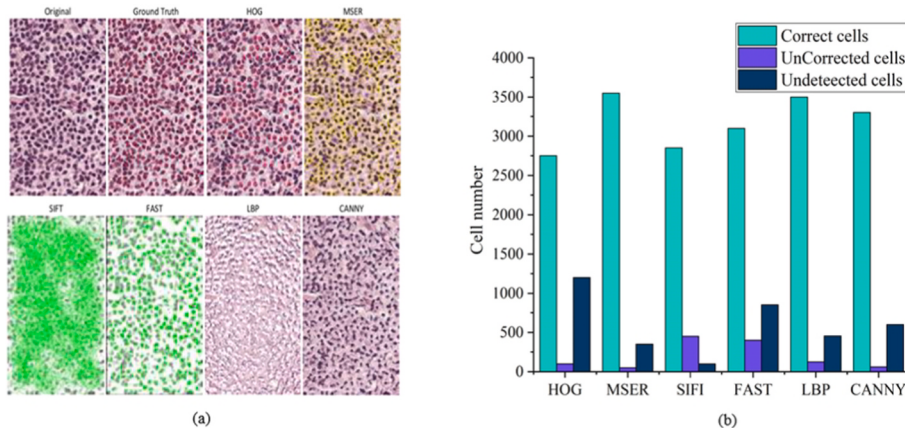


Fig. 14. Comparison of six commonly used feature extraction algorithms. (a) Features determined by feature extraction algorithms [50]. (b) Comparison of cell extraction accuracy of feature extraction methods.

4.2. Deep learning

Traditional feature extraction techniques include shape, color, and texture-based feature extraction, called handcrafted features. When these feature extraction methods are used, many issues need to be paid attention to, such as sensitivity to light intensity, quantization error, and high dimension of representation, which also leads to their low accuracy and precision. In recent years, with the widespread application of deep learning in image classification, researchers are also trying to apply neural networks to image feature extraction. For biological images, deep learning can conduct a range of feature extraction, feature optimization, and classification procedures, saving time and resources.

Based on CNN, Zheng et al. [122] suggested a kernel-guided feature extraction method for histopathology images. The sensitivity, stability and specificity of this framework were all above 95%. Yonekura et al. [123] proposed a deep convolutional neural networks (deep CNNs) to extract features from histopathological images of glioblastoma multiforme (GBM) with an average accuracy of 96.5%. Mehra et al. [124] adopted three pretrained networks: VGG16, VGG19, and ResNet-50 as feature generators, and extracted features from breast cancer histopathology images for classifiers. Experiments demonstrated that even with the limited size of the training dataset, using transfer learning method could achieve significant performance when fully trained CNNs. Inception-ResNet-V2 was proposed by Xie et al. [125] to extract features from breast cancer histopathology pictures for unsupervised analysis. The experimental results showed that the model achieved perfect consistency for binary classification of breast cancer histopathological images.

Vo et al. [126] used DCNNs model to extract visual features in breast cancer classification, and found that it was capable of extracting both global and local features of breast cancer tumors, resulting in improved classification performance for distinct breast cancer kinds. George et al. [127] applied AlexNet, ResNet-18 and ResNet-50 to merge the extracted nuclear features of a single image into global features, and obtained an accuracy of 96.88%. Kate et al. [128] adopted a three-layer CNN to extract global, local and spatial features from a given pathology image. This method helps to extract obvious feature information. Rashmi et al. [129] proposed to use BCHisto-Net to extract global and local features of breast histopathology images, and then used a feature aggregation branch to fuse global and local features, which could improve the accuracy of breast histopathology image classification. The accuracy of this method on Kasturba Medical College (KMC) and Breakhis datasets was 95% and 89% respectively, which proved the effectiveness of the extractor for accurate classification. Sharma et al. [130] used the Xception model as a feature extractor for breast cancer histopathology image classification, which provided a more robust and reliable

classification model. Kumar et al. [115] employed DenseNet, SqueezeNet, VGGNet, Xception, and ResNet-50 to extract deep features from histopathological images of lung and colon cancers. Following a thorough study, the classifier built from the characteristics retrieved by the DenseNet pre-trained network performed the best, with classification accuracy and precision for lung and colon cancer histopathology pictures exceeding 97%, as shown in Fig. 15. The DenseNet architecture was proposed by Huang et al. [131] in 2017, which could enhance feature propagation, encourage feature reuse and require fewer parameters.

4.3. Summary

The precision of feature extraction, a fundamental stage in image processing, determines the accuracy of cancer cell detection. Shape features are constant data that does not change when the environment changes. Many shape features, on the other hand, simply represent the local attributes of things, and a thorough description of objects necessitates a significant amount of computer time and storage space. Color photos are usually converted to grayscale images first, and then

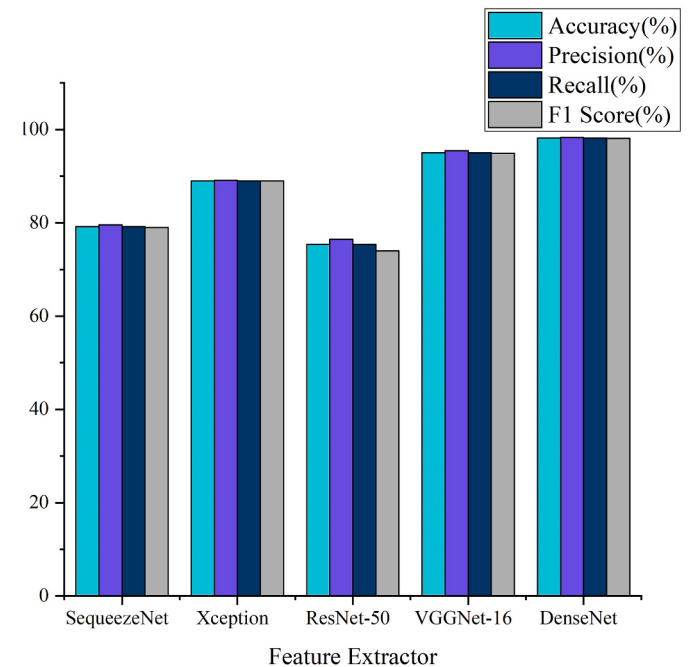


Fig. 15. Performance comparison of different feature extractors [115].

analyzed using grayscale image processing methods, because processing and analyzing color images for color features is generally hard and time-consuming. Texture feature extraction is a typical approach for extracting features from histopathological pictures. This approach has excellent anti-noise properties, although it is sensitive to light and reflection. GLCM is one of the most adaptable and resilient texture feature extraction algorithms, however it lacks global image information. In Table 4, we also address the benefits and drawbacks of feature extraction approaches. Varying feature extraction methods will provide different success rates for histopathological image features, therefore selecting relevant features is a vital aspect in improving recognition accuracy.

5. Classifier

The learning of a classification function or the construction of a classification model based on existing data is a really essential way of data mining. As a result, classifier refers to a wide range of sample

classification techniques, including closest neighbor, naive Bayes, decision tree (DT), logistic regression, support vector machine (SVM), neural network, deep learning, and others. Since the feature extraction of deep learning does not rely on manual extraction, it has received more and more attention in the automatic detection of cancer cell pathology. Therefore, this section mainly revolves around traditional machine learning classifiers and deep learning classifiers. The accuracies of different traditional classifiers are shown in Fig. 16.

5.1. Traditional classifiers

5.1.1. Decision tree (DT)

DT is a tree-structured classification algorithm and a basic classification and regression approach. The algorithm is simple to comprehend and apply, can handle a big quantity of data in a short amount of time, and produces reasonable and effective outcomes. However, this algorithm is prone to overfitting, and for data with inconsistent numbers of samples in each category, the information gain is biased towards those

Table 4
Feature extraction method of histopathological image.

Types	Methods	Authors, year	Targets	Comments
Shape features	Local double ellipse descriptors	Lu et al. (2013) [86]	Skin	Good segmentation sensitivity.
	Stiffness moment characteristics	Tashk et al. (2015) [107]	Breast	Improve classification accuracy.
Color features	Geometric features	Wang et al. (2018) [108]	Intestine	Effectively distinguish abnormal hyperplasia image from normal image.
	Color texture feature construction method based on nonlinear color quantization	Sertel et al. (2009) [110]	Lymph	Maximize the classification performance.
	Color gradient function	Xu et al. (2011) [77]	Prostate	Produce more obvious boundaries.
	Local Fourier transform	Kong et al. (2011) [111]	Lymph	The extracted color texture features have a good identification effect for classification.
	2D histograms of color distribution	Bejnordi et al. (2014) [112]	Lymph	Good image stability.
	RGB and LAB color spaces	Rashmi et al. (2020) [113]	Breast	Improve segmentation performance.
	Python	Chen et al. (2021) [114]	Stomach	To provide useful markers for the differentiation of gastric cancer.
	Color correlogram	Kumar et al. (2022) [115]	Lung, Colon	Using a single color space, there is no robust discriminant feature.
Texture features	A new color-texture analysis method	Sertel et al. (2008) [83]	Follicular lymph	It is superior to gray texture analysis and significantly improves the classification performance.
	Gabor filter	Krishnan et al. (2012) [117]	Oral cavity	The extracted features have high accuracy for classification.
	Haralick texture feature descriptor	Albayrak et al. (2013) [116]	Breast	Improve cell separation accuracy.
	LBP	Bruno et al. (2016) [118]	Breast	The ratio obtained is between 91% and 100%.
	Histogram of Oriented Gradients	Phouladhy et al. (2016) [119]	Cervix	The accuracy rate is 93.33% and the false negative rate is zero.
	Multispectral multiscale local binary model	Peyret et al. (2018) [120]	Prostate	The accuracy of the algorithm on different data sets is 99.6%.
Neural network	GLCM	Öztürk et al. (2018) [121]	Organization	It can successfully represent images with fewer parameters.
	N-CNN	Zheng et al. (2017) [122]	Breast	The sensitivity, stability and specificity are above 95%.
	Deep CNNs	Yonekura et al. (2018) [123]	Glioblastoma multiforme	Average accuracy of 96.5%.
	VGG16, VGG19, ResNet-50	Mehra et al. (2018) [124]	Breast	Can achieve remarkable performance.
	Inception-ResNet-V2	Xie et al. (2019) [125]	Breast	The model achieves perfect agreement for binary classification of breast cancer histopathology images.
	DCNN	Vo et al. (2019) [126]	Breast	Effectively extract the global and local features of tumor.
	AlexNet, ResNet-18, ResNet-50	George et al. (2019) [127]	Breast	The classification accuracy is 96.54%, 96.05% and 95.90% respectively.
	BCHisto-Net	Rashmi et al. (2021) [129]	Breast	The accuracy of this method is 95% and 89% on the KMC and BreakHis datasets, respectively.
	Xception	Sharma et al. (2022) [130]	Breast	This model provides a more robust and reliable classification model.
	DenseNet, SqueezeNet, VGGNet, Xception, ResNet-50	Kumar et al. (2022) [115]	Lung, Colon	Can enhance feature propagation, encourage feature reuse and require fewer parameters.

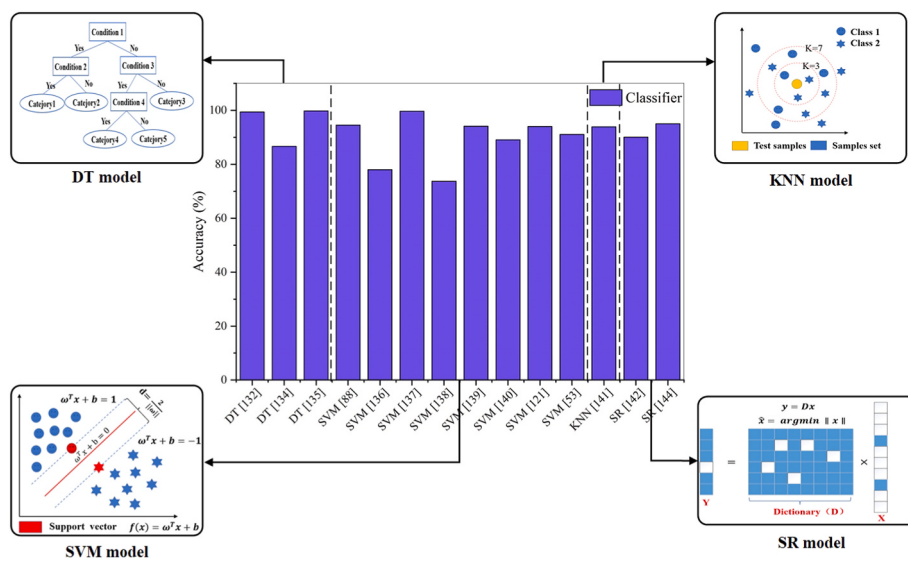


Fig. 16. Classification accuracy of traditional classifier.

with a larger number of samples. From oral histopathology images, Rahman et al. [132] retrieved shape, texture, and color features, and then used different classifiers for classification, among which, the DT classifier achieved 99.4% accuracy. Bagdigen et al. [133] also adopted the DT classifier to classify breast histopathology images. Korkmaz et al. [134] applied DT and DA classifiers to categorize stomach histology images, the accuracy of this method was 86.66%. Rahman et al. [135] proposed the DT classifier for the classification of oral squamous cells based on morphological features and texture features, and its accuracy could reach 99.78%.

5.1.2. Support vector machine (SVM)

SVM is a supervised learning method proposed by Vapnik in 1995, which can be widely used in statistical classification and regression analysis. The classification idea of the SVM algorithm is really simple, and the classification effect is good, however, for large-scale training samples, the SVM algorithm is difficult to implement, and is sensitive to the selection of missing data and parameters and functions.

Huang et al. [88] proposed an SVM-based decision graph classifier to classify hepatocellular carcinoma (HCC) biopsy images. The experimental results showed that the classification accuracy of the classifier reached 94.54%. Kuse et al. [136] used SVM to classify features extracted from lymphocytes, which could achieve a classification accuracy of 78% and a false positive rate of 14.7%. Krishnan et al. [137] adopted linear kernel-based SVM to classify texture features and intensity features extracted from oral histopathology images with up to 99.66% accuracy. Xu et al. [138] designed three commonly used methods for multi-classification: one-against-all SVM (OAA), one-against-one SVM (OAO) and multi-structure SVM. The experimental results showed that the correct rate of multi-structure SVM for the classification of colon histopathology images was 73.7%. Al-Kadi et al. [139] used SVM, Bayesian and K-nearest neighbors (KNN) classifiers to classify meningioma brain histopathology images. After testing, the overall classification accuracy of SVM, Bayesian and KNN classifiers was 94.12%, 92.50% and 79.70% respectively. Masood et al. [140] applied an efficient self-suggestion version of SVM to evaluate and classify histopathological images with an average diagnostic accuracy of 89.1%. Öztürk et al. [121] proposed SVM, KNN, LDA and boosting tree classifiers to classify features extracted from histopathological image textures, and then compared the performance of each classifier. The experimental results showed that among the classification algorithms, the SVM and boosting tree classifier algorithms had the highest success rates (94%, 94.3%). SVM was employed by Aswathy et al. [53] to categorize benign

and malignant breast cancer histopathology images, and the classifier reached 91.1% accuracy after analysis.

5.1.3. K-nearest neighbors (KNN)

When the data and labels in the training set are known, the KNN algorithm compares the features of the test data with the corresponding features in the training set, and finds the top k data in the training set that is the most comparable. The category corresponding to the data is the category with the most occurrences in the k data. The algorithm is simple, easy to understand and implement, does not require parameter estimation, and is suitable for multi-classification problems; however, the amount of calculation required is excessive, especially when the number of features is large; each text to be classified must be calculated to the whole. Knowing the distance of the sample can get its Kth nearest neighbor point. Niwas et al. [141] used the KNN algorithm to classify the extracted breast histopathology image features, and its classification accuracy reached 93.9%.

5.1.4. Sparse representation (SR)

The term “sparse representation” refers to the process of representing most or all of the original signals using a linear combination of fewer basic signals. The basic signals are known as atoms and are chosen from an over-complete dictionary; the over-complete dictionary is made up of the number of Atoms that surpass the signal’s dimension and is aggregated. Han et al. [142] suggested a dictionary learning and sparse coding-based automatic tissue classification system, which compared the performance of the classifier with SVM and KDA, and the data showed that on 3-class problem, the classification accuracy of SR was 90.05%, with 85.87% accuracy on 4-class problem. Shirale et al. [143] used a sparse representation-based class-level dictionary learning method for histopathology image classification, which reduced pathologists’ workload and produced good results on a variety of histopathology image datasets, with an accuracy rate of up to 96.56%. Li et al. [144] employed a mutual information-based multi-channel joint sparse model. The MIMCJSM model used the mutual information criteria to build a common sub-dictionary and three specific sub-dictionaries to encode the common components and specific components, respectively, which improved the recognition ability of joint sparse coding. The method had good classification performance and robustness, and its classification accuracy for lung histopathology images could reach more than 95%.

5.2. Deep learning

5.2.1. Convolutional neural network (CNN)

The neural network has a high classification accuracy, powerful parallel distribution processing and learning ability, good robustness and fault tolerance to noisy nerves. Then it can fully approximate complicated nonlinear relationships, and has an associative memory function. However, neural networks require a vast number of parameters, such as network architecture, initial weights, and thresholds; the learning process cannot be witnessed, and the output findings are difficult to explain, affecting the results' credibility and acceptability. If the training time is too long, it may not even achieve the goal of study. Neural networks commonly used in histopathological image classification include CNN, AlexNet, ResNet and VGGNet.

Stanitsas et al. [145] used the AlexNet to classify pathological images, which greatly reduced the requirements for graphics processing unit memory, thus avoiding the need for complex hardware. Zheng et al. [146] proposed a kernel-guided feature extraction framework based on CNN for the representation and classification of breast histopathology images with an average classification accuracy of 96.4%. Han et al. [147] adopted GoogleNet to significantly improve the classification performance through 22 layers deep network and novel initial module. Bejnordi et al. [148] had trained a 11 layers VGG class CNN, which could distinguish breast cancer from normal breast tissue from matrix tissue. Gandomkar et al. [149] used ResNet to classify breast histopathological images in multiple categories, and the classification accuracy reached 96.25%. Öztürk et al. [150] proposed a whole-slide histopathological image classification network (HIC-net) based on CNN. The author used a large dataset to evaluate the HIC-net algorithm, and the AUC score of HIC-net was 97.7%; using the softmax function to evaluate the HIC-net, the accuracy reached 96.21%, the sensitivity reached 96.71%, and the specificity reached 95.7%. Saito et al. [151] trained a CNN with 30,584 wireless capsule endoscopy images of prominent lesions, and its sensitivity and specificity were 90.7% and 79.8%, respectively, and the detection rate of prominent lesions was 98.6%. Panigrahi et al. [152] proposed a new method called capsule network deep learning technique to classify oral cancer histopathology images, the classification sensitivity of this method was 97.78%, specificity was 96.92%, and accuracy was 97.35%. Kumar et al. [153] proposed a VGGNet-16 based framework, which had an average accuracy rate of 97% for human breast cancer based on the two element classification.

Burçak et al. [154] proposed a DCNN model to classify breast cancer histopathology images. Experiments showed that the model was an efficient classification model with an accuracy rate of 99.05%. Rashmi et al. [129] adopted to classify $100\times$ magnified breast histopathology images with BCHisto-Net, a novel CNN architecture. BCHisto-Net was quantitatively evaluated on the KMC dataset with an accuracy of 95%. To categorize breast cancer histopathology pictures, Gupta et al. [155] employed an improved residual neural network-based technique. On the BreakHis dataset, with a precision of 99.18% and a recall rate of 99.37%, the approach achieved an average classification accuracy of 99.75% at $40\times$ magnification. Combining with the merits of CNN and capsule network (CapsNet), Wang et al. [156] applied a deep feature fusion and enhanced routing (FE-BkCapsNet) algorithm for breast cancer histopathological image classification. After testing on the BreakHis dataset, the image classification accuracy rates of different magnifications were: 92.71% for $40\times$, 94.52% for $100\times$, 94.03% for $200\times$, 93.54% for $400\times$. Su et al. [157] proposed a new semi-supervised CNN method called Semi-HIC, which improved classification performance by using a large number of unlabeled histopathology images. Experiments showed that this strategy consistently beat semi-supervised LA methods and outperformed existing deep learning algorithms in histopathology classification. Yan et al. [158] employed a hybrid convolutional deep neural network (DNN) for breast cancer histopathology image classification, which incorporated the benefits of convolutional and recurrent neural networks and achieved an average classification accuracy of

91.3%. Joseph et al. [159] adopted hand-crafted feature extraction techniques to extract color, shape, and texture features, and then used a DNN to classify breast histopathology images on the BreakHis dataset in histopathology images at different magnifications. All had high accuracy: 97.87% for $40\times$, 97.60% for $100\times$, 96.10% for $200\times$, 96.84% for $400\times$. Chattopadhyay et al. [160] created the dense residual dual-shuffle attention network, a dual-shuffle attention-guided deep learning model (DRDA-Net). The model addressed overfitting and vanishing gradients. After evaluation on the public BreakHis dataset, its classification accuracies at $40\times$, $100\times$, $200\times$, and $400\times$ magnification were 95.72%, 94.10%, 97.43%, and 98.1%, respectively. Wang et al. [161] proposed a dependency-based lightweight convolutional neural network (DBLCNN) to classify breast histopathology images, as shown in Fig. 17. The technique had state-of-the-art results in terms of recognition performance and computing utilization, according to its experimental results on the BreakHis dataset, with an image-level accuracy of 96% and a patient-level accuracy of 97.59%.

With the proposal of more and more network architectures, some older networks gradually fade out of people's vision, but the logic and ideas behind them are worth learning. The design principle of CNN architecture is that the greater the depth of the network, the higher the accuracy. The network structure tends to use fewer convolution cores to improve the computational efficiency. The module structure may become popular in the future, and as GoogleNet and ResNet demonstrate, it is an effective design strategy. The network's design space can be reduced thanks to the modular construction. Using the bottleneck layer in the module, on the other hand, can lower the amount of computation.

5.2.2. Generative adversarial network (GAN)

One of the most promising approaches for unsupervised learning on complicated distributions in recent years has been the GAN, a deep learning model. The mutual game learning of the generative model and the discriminative model in the framework allows the model to deliver good results. Jaiswal et al. [162] proposed a capsule network-based generative adversarial network (CapsuleGAN). Experiments showed that CapsuleGAN was superior to convolutional GAN, and its generated images were closer to real images, more diverse, and had better semi-supervision on test datasets Classification performance. To address the problem of mislabeling and improve classification performance, Man et al. [163] adopted a novel breast histopathology classification method that used generative adversarial networks and convolutional networks to screen mislabeled patches and extract features, as shown in Fig. 18. The method achieved the best accuracy of 99.13% on the BreakHis dataset. Wang et al. [164] used a prototype transfer generative adversarial network as an unsupervised learning method (PTGAN) in order to solve the problem of supervised learning relying on a large amount of labeled data, which saved the cost of complex labeling and had a significant impact on breast cancer. The classification accuracy of benign and malignant histopathology images was close to 90%. Xue et al. [165] applied a HistoGAN model for synthesizing cervical cancer histopathology images, and selectively added the real samples generated by HistoGAN to the original dataset, improving the classification performance. Li et al. [166] proposed a multi-scale conditional GAN to generate high-resolution and large-scale histopathology images, which solved the problem of data limitation and improved the segmentation and classification performance.

5.2.3. Domain adaptation

Domain adaptation is to achieve the effect that the performance of the model in another domain approximates or even remains in the original domain. Alirezazadeh et al. [167] suggested a new unsupervised adaptive technique for classifying breast histopathology images based on representation learning. This method addressed the deficiencies of histological image-based computer aided diagnosis systems and the similarity of benign and malignant images, with an average

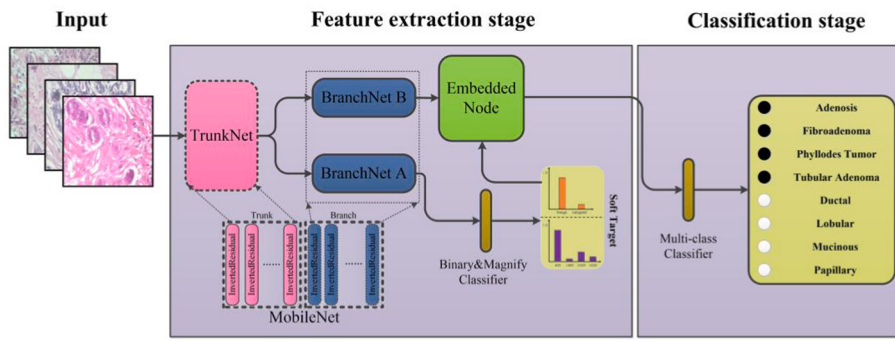


Fig. 17. Overview of the DBLCNN for multi-classification of breast histology images [161].

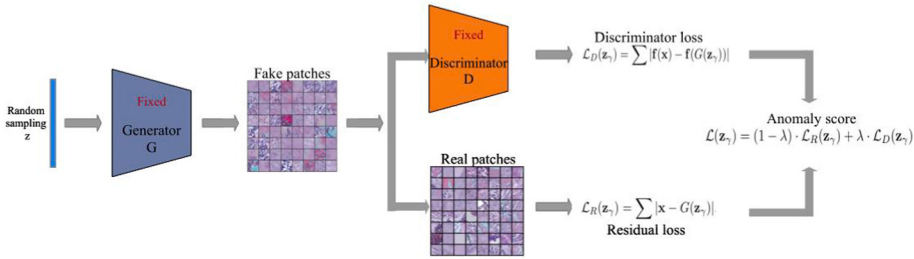


Fig. 18. The framework of screening patches from anomaly detection with generative adversarial networks (AnoGAN) (Generative adversarial training is performed on benign data and testing is performed on both, unseen healthy cases and anomalous data) [163].

classification rate of 88.5% on the BreakHis dataset. Yu et al. [168] introduced unsupervised adaptation in a deep convolutional neural network model to reduce label duplication, which did not require recall of large-scale labeled data for each specified domain. Experiments showed that the accuracy of this method was higher than 90%. Figueira et al. [169] applied an adversarial-based domain adaptation network (ABDA-Net) for tumor detection in histopathology with an accuracy of up to 93.53%. Wang et al. [170] used a deep transfer semi-supervised domain adaptation model (HisNet-SSDA) to classify histopathology slide images. Semi-supervised domain adaptation could transfer information from a source domain to a partially labeled target domain, align the features of the two domains, aggregate the projected probability of sampled patches, and then classify the results. The method achieved 94.32% accuracy in classifying histopathological images of colon cancer.

5.2.4. Principal component analysis network (PCANet)

In machine learning, data is usually represented as a vector and input to the model for training, but direct processing and analysis of a large amount of multidimensional data will consume a lot of system resources, so dimensionality reduction is needed to alleviate this problem. Dimensionality reduction is to use a low-latitude vector to represent the features of the original high-latitude vector. Principal component analysis is a common dimensionality reduction method. Principal component analysis transforms a set of potentially correlated variables into a set of linearly uncorrelated variables through an orthogonal transformation. Principal component analysis is an unsupervised method, without classification labels, its calculation is simple, and there is no parameter limitation, but it cannot intervene in the processing process through parametric methods.

Sertel et al. [110] utilized a Bayesian classifier to classify follicular lymphoma histopathology images with an accuracy of 88.9% after combining principal component analysis and linear discriminant analysis to reduce the dimensionality of the feature space. Shi et al. [171] adopted a PCANet algorithm based on random binary hashing of color patterns, which performed cascaded principal component analysis on

the principal component images of three color channels, R, G, and B, to extract the color modulus and the angle modulus, as shown in Fig. 19. The feature learning and classification framework integrating C-RBH-PCANet with a matrix-form classifier got the best results in the experiments. Mukkamala et al. [172] proposed a framework for analyzing color histopathology images using PCANet and then using support vector machines to classify the features of the extracted breast

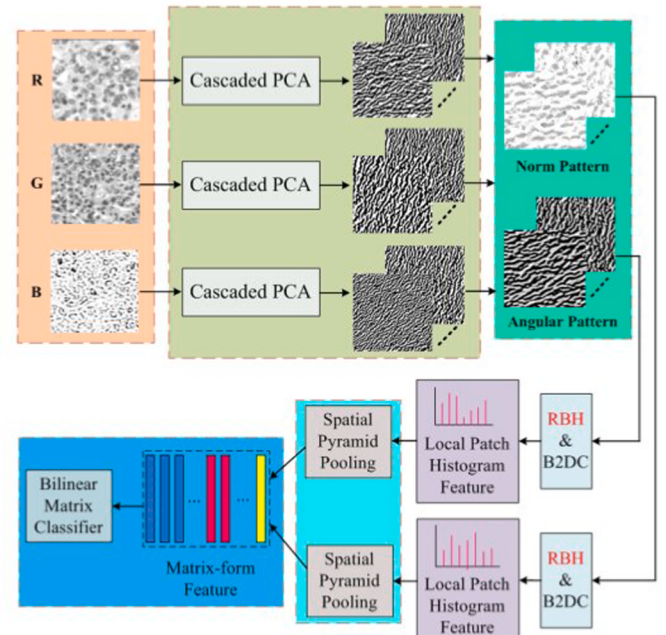


Fig. 19. The color pattern random binary hashing based PCANet flow chart and color histopathological image classification framework based on matrix classifier [171].

cancer histopathology images. Compared with the traditional breast tumor classification method, the method was significantly improved, and its accuracy rate reached 97%. Shi et al. [173] embedded the genetic algorithm into the PCANet framework and proposed a quaternion-based Grassmann average network algorithm (QGANet). The experimental results showed that the QGANet algorithm had the best classification performance for color histopathological images, with an average classification accuracy of 90%, a sensitivity of 89.84%, and a specificity of 94.93%. Zhang et al. [174] used a non-Hodgkin lymphoma subtype classification method that fused transfer learning (TL) and PCA. The experimental results showed that the overall classification accuracy of this method was 98.93%.

5.3. Summary

Currently, pathological image classification accuracy is typically above 85% (as shown in Table 5), which appears to be good yet unstable. As illustrated in Fig. 20, the classification results of many research may only apply to the study samples, and the classification accuracy of various sample sets may vary substantially. The characteristics chosen have a significant influence on categorization accuracy. For feature extraction, Fourier transform mass spectrometry was used by Korkmaz et al. [134]. The maximum accuracy rate was 86.66% when five features were picked; the greatest accuracy rate was 68.88% when the number of specified criteria was increased to 45. As a result, it's worth considering how to identify relevant qualities and the generality of classification methods. Traditional machine learning classifiers are the most common image classification approach, and while they can produce predicted classification results based on users' demands, they are influenced by subjective elements to some extent. In the categorization process, deep learning does not require any prior knowledge; it may learn from a large number of training examples, identify some hidden rules, and then categorize the images. Traditional machine learning classifiers are dominant, but classification without deep learning does not rely on past information, can learn spontaneously, and has transfer learning capabilities, all of which have enormous development potential.

6. Discussion

Due to the improvement of medical conditions, the traditional manual methods are increasingly unable to meet the identification requirements of massive medical images. With the continuous improvement of machine vision technology, intelligent detection based on machine vision is more and more widely used in various industries in today's society. Therefore, the application of intelligent technology in medicine has become extremely urgent, especially histopathological image detection has played a really important auxiliary role in cancer detection and has become the mainstream cancer cell detection method. In actual medical testing, histopathological image detection methods are generally not applied to clinical diagnosis alone, but should also be combined with other detection methods, such as CT, MRI, and positron emission tomography (PET), for more accurate diagnosis. This also puts forward new requirements for the fusion diagnosis of multiple medical images in the future.

In the medical field, image segmentation is the basis for lesion region extraction and subsequent automatic identification. However, medical images obtained due to various reasons inevitably have characteristics such as blur and unevenness. Therefore, image segmentation techniques are of great significance in medical image processing and are still the hotspot of current medical image processing. Automatic detection of various cancer cells is still in the exploratory stage, according to present research, and detection accuracy needs to be increased in comparison to people. This requires the combination of the powerful computing power of the computer system and the subjective ability of pathologists, which will greatly improve the efficiency and accuracy of clinical diagnosis. Furthermore, a greater focus on the automated detection of low-

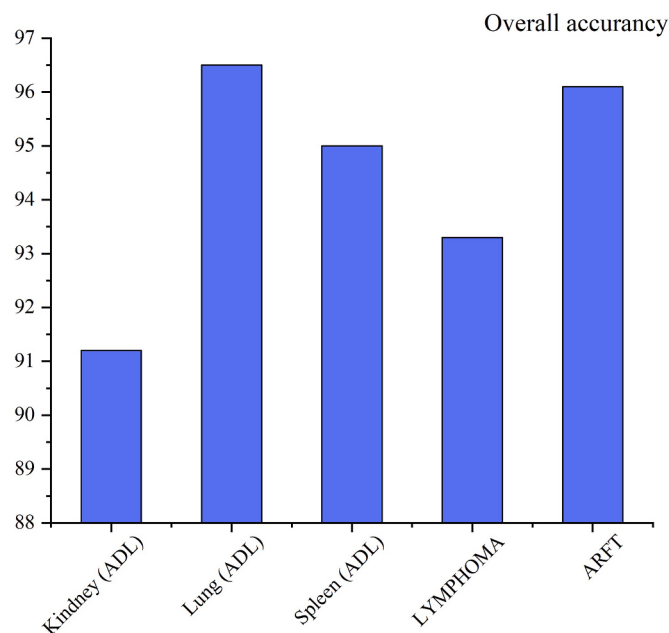
Table 5
Classification methods for histopathological images.

Type	Method	Authors, year	Targets	Accuracy
Traditional classifier	DT	Korkmaz et al. (2018) [134]	Gastric	86.66%
	DT	Rahman et al. (2020) [132]	Oral	99.4%
	DT	Rahman et al. (2020) [135]	Oral	99.78%
	SVM	Huang et al. (2010) [88]	Liver	94.54%
	SVM	Kuse et al. (2010) [136]	Lymph	78%
	SVM	Krishnan et al. (2012) [137]	Oral	99.66%
	SVM	Xu et al. (2013) [138]	Colon	73.7%
	SVM	Al-Kadi et al. (2015) [139]	Brain	94.12%
	SVM	Masood et al. (2015) [140]	Skin	89.1%
	SVM	Öztürk et al. (2018) [121]	Organization	94%
	SVM	Aswathy et al. (2020) [53]	Breast	91.1%
	KNN	Niwas et al. (2013) [141]	Breast	93.9%
	SR	Han et al. (2011) [142]	Brain	90.05%
	SR	Shirale et al. (2018) [143]	ADL dataset, Lymphoma dataset, ARFT	96.11%
	SR	Li et al. (2020) [144]	ADL dataset, BreaKHis datasets	Average accuracy over 90%
	AlexNet	Stanitsas et al. (2016) [145]	Breast, Prostate	92.83%, 91.51%
	CNN	Zheng et al. (2017) [146]	Breast	96.4%
Deep learning	GoogleNet	Han et al. (2017) [147]	Breast	93.2%
	VGG	Bejnordi et al. (2017) [148]	Breast	95.5%
	ResNet	Gandomkar et al. (2018) [149]	Breast	96.25%
	HIC-Net	Öztürk et al. (2019) [150]	Organization	96.21%
	CNN	Saito et al. (2020) [151]	Intestine	98.6%
	Capsule Network	Panigrahi et al. (2020) [152]	Oral	97.35%
	VGGNet-16	Kumar et al. (2020) [153]	Breast	97%
	DCNN	Burçak et al. (2021) [154]	Breast	99.05%
	BCHisto-Net	Rashmi et al. (2021) [129]	Breast	95%
	ResNet	Gupta et al. (2021) [155]	Breast	99.75%
	FE-BkCapsNet	Wang et al. (2021) [156]	Breast	94.52%
	DNN	Yan et al. (2020) [158]	Breast	91.3%
	DNN	Joseph et al. (2022) [159]	Breast	97.87%
	DRDA-Net	Chattopadhyay et al. (2022) [160]	BreakHis datasets	98.1%
	DBLCNN	Wang et al. (2022) [161]	Breast	97.57%
	GAN	Man et al. (2020) [163]	Breast	99.13%
	GAN	Wang et al. (2021) [164]	Breast	90%

(continued on next page)

Table 5 (continued)

Type	Method	Authors, year	Targets	Accuracy
Domain adaptation	Alirezazadeh et al. (2018) [167]	BreakHis dataset		
Domain adaptation	Figueira et al. (2020) [169]	Tumour	93.53%	
Domain adaptation	Wang et al. (2022) [170]	Colon	94.32%	
PCA	Shi et al. (2016) [171]	ADL dataset	81.8%	
PCA	Mukkamala et al. (2018) [172]	Breast	97%	
PCA	Shi et al. (2019) [173]	HCC dataset	94.58%	
PCA	Zhang et al. (2020) [174]	Lymph	98.93%	

**Fig. 20.** Classification accuracy of histopathological image classification method based on SR for different data sets [143].

incidence malignancies is conducive to the development of a comprehensive machine vision-based cancer cell detection system. At the moment, many researchers' techniques or models can only detect certain types of cancer cells, and they lack the ability to transmit knowledge. When these technologies are forcibly transplanted to the detection of other types of cancer cells, the detection accuracy is similarly low and unstable, necessitating further investigation.

The machine vision cancer detection process includes image pre-processing, target region segmentation, feature extraction and selection, cell recognition, and classification. In each processing activity, several algorithms emerge, each with its own set of benefits and drawbacks, as well as a range of adaptability. Researchers have long been interested in how to increase the algorithm's accuracy, execution efficiency, real-time responsiveness, and resilience. In addition, with the rapid development of deep computer technology, machine learning and deep learning methods are increasingly used in radiomics research. Most applications of traditional machine learning in medical imaging rely on supervised machine learning methods, which means that a lot of data calibration needs to be done manually. For cancer cell detection, the feature extraction of traditional machine learning mainly relies on manual work. Manual feature extraction is simple and effective for specific

simple tasks, but it is not universal. The feature extraction of deep learning does not rely on humans, but is automatically extracted by machines. Compared with traditional machine learning, deep learning has strong learning ability, good portability, and high prediction accuracy, but it has a large amount of calculation, poor portability, complex model design, and prone to bias. This is because a deep learning model is effectively a black box that does not give interpretability of the decision-making process, making debugging difficult when it is required. Poor interpretability may cause doctors who are educated to interpret clinical findings to be distrusted. The creation of a generic interpretable framework for medical image processing might be a future trend.

7. Outlook

Because machine vision can quickly process a large amount of data and is easy to process automatically, people gradually apply machine vision widely in manufacturing, pharmaceutical industry, astronomy industry, transportation and navigation industry, military industry and so on. In recent years, machine vision has become more and more widely used in medical systems. Machine vision is usually used in medical imaging diagnosis to assist doctors and improve the efficiency of doctors' diagnosis. Machine vision algorithms have greatly improved the accuracy of cancer cell detection, but the accuracy of machine vision algorithms is difficult to reach 100%, and there are still some shortcomings. Therefore, we still need to continuously improve the detection method of cancer cells based on machine vision. For future research, we can focus on the following aspects.

- (1) Histopathology detection systems need to be standardized to reduce systematic and random errors due to equipment variation. The detection system based on machine vision is composed of multiple links. As long as there is a problem in one link, the detection error will increase layer by layer, which is a problem worthy of attention. On the other hand, unifying data from different sources to minimize the complexity created by the detection process. To judge the accuracy of the detection algorithm, it is necessary to use the datasets to conduct experiments. The larger the datasets, the more reliable the experimental results. Although there are more and more datasets on histopathological images in recent years, there is no unified standard, and experiments are often performed on different datasets, which makes the experimental process more complicated, and the actual detection process of cancer cells is also more complicated. Data formats and data analysis criteria in different datasets should be normalized to reduce errors during detection.
- (2) Investigate more stable algorithms to improve image processing and recognition capabilities. In the process of cancer cell detection, it is necessary to reduce the computational complexity and improve the accuracy. Optimize traditional vision methods to make them more flexible and reduce inspection time. Improve the robustness of traditional vision methods, and solve the problems of complex parameter adjustment and difficulty in getting started with traditional algorithms. Scientifically and accurately evaluate the efficiency and performance of traditional vision algorithms. In addition, when detecting cancer cells in the future, it is necessary to integrate traditional vision methods and depth vision methods, and combine the advantages of both to detect cancer cells more accurately and efficiently.
- (3) Although DNNs have high accuracy and stability in histopathological detection. However, because the decision-making process of deep learning is incomprehensible to humans, it is frequently referred to as a black box. People are curious about the internal decision-making process of deep learning because their decision-making process is typically a white box. This will boost deep learning research online. Many researchers have tried to explain the black box problem and have tried to provide solutions [175].

- (4) Machine vision algorithms need to be fully validated using a large number of different datasets to assess the applicability of the method before they can be applied to the clinic. Based on the data used by deep learning methods, it is divided into training set and validation set, and try to use independent test set for validation. A key objective of deep learning methods is to ensure that these methods generalize well enough to adequately respond to various contingencies during the treatment phase. On the other hand, multiple auxiliary diagnostics are used for cancer detection to reduce the error rate.

Declaration of competing interest

The authors declare that they have no known competing financial interests or personal relationships that could have appeared to influence the work reported in this paper.

Acknowledgements

This research was also supported by Key scientific and technological projects in Henan Province in 2020 (Grant No.202102210395) and Scientific and Technological Innovation Team of Colleges and Universities in Henan Province in 2020 (Grant No.20IRTSTHN015). In addition, this research was also supported by the Local Innovative and Research Teams Project of Guangdong Pearl River Talents Program (2017BT01G167). Wenbin He, Ting Liu and Yongjie Han contributed equally to this review and are co-first authors. The two corresponding authors, Wuyi Ming and Yuan Yang, are also co-corresponding authors.

References

- [1] P. Vineis, C.P. Wild, Global cancer patterns: causes and prevention, *Lancet* 383 (9916) (2014) 549–557.
- [2] C.E. DeSantis, K.D. Miller, A. Goding Sauer, A. Jemal, R.L. Siegel, Cancer statistics for african americans, *CA A Cancer J. Clin.* 69 (3) (2019) 211–233, 2019.
- [3] F. Bray, J. Ferlay, I. Soerjomataram, R.L. Siegel, L.A. Torre, A. Jemal, Global cancer statistics 2018: globocan estimates of incidence and mortality worldwide for 36 cancers in 185 countries, *CA A Cancer J. Clin.* 68 (6) (2018) 394–424.
- [4] W. Cao, H.-D. Chen, Y.-W. Yu, N. Li, W.-Q. Chen, Changing profiles of cancer burden worldwide and in China: a secondary analysis of the global cancer statistics 2020, *Chinese Med J* 134 (2021) 783–791, 07.
- [5] L.E. Hipp, B.B. Hulswit, K.J. Milliron, Clinical Tools and Counseling Considerations for Breast Cancer Risk Assessment and Evaluation for Hereditary Cancer Risk, *Best Practice & Research Clinical Obstetrics & Gynaecology*, 2022.
- [6] M. Iranifam, Analytical applications of chemiluminescence methods for cancer detection and therapy, *Trac. Trends Anal. Chem.* 59 (2014) 156–183.
- [7] G. Logambal, V. Saravanan, Cancer Diagnosis Using Automatic Mitoic Cell Detection and Segmentation in Histopathological Images, 2015, pp. 128–132.
- [8] Cancer tomorrow. <https://gco.iarc.fr/tomorrow>. (Accessed 28 February 2022).
- [9] J.A. Seibert, One hundred years of medical diagnostic imaging technology, *Health Phys.* 69 (5) (1995) 695–720.
- [10] Y. Zhang, L. Wei, J. Li, Y. Zheng, X. Li, Status quo and development trend of breast biopsy technology, *Gland Surg.* 2 (1) (2013) 15.
- [11] L. He, L.R. Long, S. Antani, G.R. Thoma, Histology image analysis for carcinoma detection and grading, *Comput. Methods Progr. Biomed.* 107 (3) (2012) 538–556.
- [12] P. Kleczek, J. Jaworek-Korjakowska, M. Gorgon, A novel method for tissue segmentation in high-resolution h&e-stained histopathological whole-slide images, *Comput. Med. Imag. Graph.* 79 (2020), 101686.
- [13] J.N. Weinstein, E.A. Collisson, The cancer genome atlas pan-cancer analysis project, *Nat. Genet.* 45 (10) (2013) 1113–1120.
- [14] P.W. Hamilton, P.J. Van Diest, R. Williams, A.G. Gallagher, Do we see what we think we see? the complexities of morphological assessment, *J. Pathol.: J. Pathol. Soc. G. B. Ireland* 218 (3) (2009) 285–291.
- [15] L.A. Teot, R. Spoto, A. Khayat, S. Qualman, G. Reaman, D. Parham, The problems and promise of central pathology review: development of a standardized procedure for the children's oncology group, *Pediatr. Dev. Pathol.* 10 (3) (2007) 199–207.
- [16] J.G. Elmore, G.M. Longton, P.A. Carney, B.M. Geller, T. Onega, A.N. Tosteson, H. D. Nelson, M.S. Pepe, K.H. Allison, S.J. Schnitt, et al., Diagnostic concordance among pathologists interpreting breast biopsy specimens, *JAMA* 313 (11) (2015) 1122–1132.
- [17] P. Wang, X. Hu, Y. Li, Q. Liu, X. Zhu, Automatic cell nuclei segmentation and classification of breast cancer histopathology images, *Signal Process.* 122 (2016) 1–13.
- [18] M. De Bruijne, Machine learning approaches in medical image analysis: from detection to diagnosis, *Med. Image Anal.* 33 (2016) 94–97.
- [19] W. He, Z. Jiang, W. Ming, G. Zhang, J. Yuan, L. Yin, A critical review for machining positioning based on computer vision, *Measurement* 184 (2021), 109973.
- [20] M. Narwaria, Does explainable machine learning uncover the black box in vision applications? *Image Vis Comput.* 118 (2022), 104353.
- [21] N. Sharma, R. Sharma, N. Jindal, Machine learning and deep learning applications-a vision, *Global Trans. Proc.* 2 (1) (2021) 24–28.
- [22] M.L. Smith, L.N. Smith, M.F. Hansen, The quiet revolution in machine vision-a state-of-the-art survey paper, including historical review, perspectives, and future directions, *Comput. Ind.* 130 (2021), 103472.
- [23] M.N. Gurcan, L.E. Boucheron, A. Can, A. Madabhushi, B. Yener, Histopathological image analysis: a review, *IEEE Rev. Biomed. Eng.* 2 (2009) 147–171.
- [24] D. Komura, S. Ishikawa, Machine learning methods for histopathological image analysis, *Comput. Struct. Biotechnol. J.* 16 (2018) 34–42.
- [25] A. Das, M.S. Nair, S.D. Peter, Computer-aided histopathological image analysis techniques for automated nuclear atypia scoring of breast cancer: a review, *J. Digit. Imag.* 33 (5) (2020) 1091–1121.
- [26] A. Korzynska, L. Roszkowiak, J. Zak, K. Siemion, A review of current systems for annotation of cell and tissue images in digital pathology, *Biocybern. Biomed. Eng.* 41 (4) (2021) 1436–1453.
- [27] N. Tomita, B. Abdollahi, J. Wei, B. Ren, A. Suriawinata, S. Hassanpour, Attention-based deep neural networks for detection of cancerous and precancerous esophagus tissue on histopathological slides, *JAMA Netw. Open* 2 (11) (2019) e1914645–e1914645.
- [28] Y. Zeng, J. Zhang, A machine learning model for detecting invasive ductal carcinoma with google cloud automl vision, *Comput. Biol. Med.* 122 (2020), 103861.
- [29] D.G. Vinsard, Y. Mori, M. Misawa, S.-e. Kudo, A. Rastogi, U. Bagci, D.K. Rex, M. B. Wallace, Quality assurance of computer-aided detection and diagnosis in colonoscopy, *Gastrointest. Endosc.* 90 (1) (2019) 55–63.
- [30] O. Kott, D. Linsley, A. Amin, A. Karagounis, C. Jeffers, D. Golijanin, T. Serre, B. Gershman, Development of a deep learning algorithm for the histopathologic diagnosis and gleason grading of prostate cancer biopsies: a pilot study, *Eur. Urol. Focus* 7 (2) (2021) 347–351.
- [31] G. Meijer, J. Beliën, P. Van Diest, J. Baak, Origins of...image analysis in clinical pathology, *J. Clin. Pathol.* 50 (5) (1997) 365.
- [32] M.D. Zarella, D. Bowman, F. Aeffner, N. Farahani, A. Xthona, S.F. Absar, A. Parwani, M. Bui, D.J. Hartman, A practical guide to whole slide imaging: a white paper from the digital pathology association, *Arch. Pathol. Lab Med.* 143 (2) (2019) 222–234.
- [33] M. García Rojo, A.M. Castro, L. Gonçalves, Cost action “euroteopath”: digital pathology integration in electronic health record, including primary care centres 6 (1) (2011) 1–5.
- [34] T.L. Sellaro, R. Filkins, C. Hoffman, J.L. Fine, J. Ho, A.V. Parwani, L. Pantanowitz, M. Montalto, Relationship between magnification and resolution in digital pathology systems, *J. Pathol. Inf.* 4 (2013).
- [35] M. Humphries, P. Maxwell, M. Salto-Tellez, Qupath: the global impact of an open source digital pathology system, *Comput. Struct. Biotechnol. J.* 19 (2021) 852–859.
- [36] N. Stathnikos, T.Q. Nguyen, C.P. Spoto, M.A. Verdaasdonk, P.J. van Diest, Being fully digital: perspective of a Dutch academic pathology laboratory, *Histopathology* 75 (5) (2019) 621–635.
- [37] G. Campanella, M.G. Hanna, L. Geneslaw, A. Miraflor, V. Werneck Krauss Silva, K. J. Busam, E. Brogi, V.E. Reuter, D.S. Klimstra, T.J. Fuchs, Clinical-grade computational pathology using weakly supervised deep learning on whole slide images, *Nat. Med.* 25 (8) (2019) 1301–1309.
- [38] T. Qaiser, A. Mukherjee, C. Reddy Pb, S.D. Munugoti, V. Tallam, T. Pitkäaho, T. Lehtimäki, T. Naughton, M. Berseth, A. Pedraza, et al., Her 2 challenge contest: a detailed assessment of automated her 2 scoring algorithms in whole slide images of breast cancer tissues, *Histopathology* 72 (2) (2018) 227–238.
- [39] N. Coudray, P.S. Ocampo, T. Sakellaropoulos, N. Narula, M. Smuderl, D. Fenyö, A. L. Moreira, N. Razavian, A. Tsirigos, Classification and mutation prediction from non-small cell lung cancer histopathology images using deep learning, *Nat. Med.* 24 (10) (2018) 1559–1567.
- [40] H.D. Couture, L.A. Williams, J. Gerardts, S.J. Nyante, E.N. Butler, J. Marron, C. M. Perou, M.A. Troester, M. Niethammer, Image analysis with deep learning to predict breast cancer grade, er status, histologic subtype, and intrinsic subtype, *NPJ Breast Cancer* 4 (1) (2018) 1–8.
- [41] D.F. Steiner, P.-H.C. Chen, C.H. Mermel, Closing the translation gap: Ai applications in digital pathology, *Biochim. Biophys. Acta Rev. Canc* 1875 (1) (2021), 188452.
- [42] S. Kobayashi, J.H. Saltz, V.W. Yang, State of machine and deep learning in histopathological applications in digestive diseases, *World J. Gastroenterol.* 27 (20) (2021) 2545.
- [43] S. Ai, C. Li, X. Li, T. Jiang, M. Grzegorzek, C. Sun, M.M. Rahaman, J. Zhang, Y. Yao, H. Li, A state-of-the-art review for gastric histopathology image analysis approaches and future development, *BioMed Res. Int.* 2021 (2021).
- [44] M. Saha, R. Mukherjee, C. Chakraborty, Computer-aided diagnosis of breast cancer using cytological images: a systematic review, *Tissue Cell* 48 (5) (2016) 461–474.
- [45] J.M. Kocarnik, K. Compton, F.E. Dean, W. Fu, B.L. Gaw, J.D. Harvey, H. J. Henrikson, D. Lu, A. Pennini, R. Xu, et al., Cancer incidence, mortality, years of life lost, years lived with disability, and disability-adjusted life years for 29 cancer groups from 2010 to 2019: a systematic analysis for the global burden of disease study 2019, *JAMA Oncol.* 8 (3) (2022) 420–444.

- [46] O. Sertel, U.V. Catalyurek, H. Shimada, M.N. Gurcan, Computer-aided Prognosis of Neuroblastoma: Detection of Mitosis and Karyorrhexis Cells in Digitized Histological Images, 2009, pp. 1433–1436.
- [47] P. Faridi, H. Danyali, M.S. Helfroush, M.A. Jahromi, Cancerous Nuclei Detection and Scoring in Breast Cancer Histopathological Images, 2016 arXiv preprint arXiv:1612.01237.
- [48] S. Özürk, B. Akdemir, Effects of histopathological image pre-processing on convolutional neural networks, *Procedia Comput. Sci.* 132 (2018) 396–403.
- [49] G. Logambal, V. Saravanan, Cancer Diagnosis Using Automatic Mitotic Cell Detection and Segmentation in Histopathological Images, 2015, pp. 128–132.
- [50] S. Özürk, A. Bayram, Comparison of hog, msmer, sift, fast, lbp and canny features for cell detection in histopathological images, *Helix* 8 (3) (2018) 3321–3325.
- [51] M. Kowal, P. Filipczuk, A. Obuchowicz, J. Korbicz, R. Monczak, Computer-aided diagnosis of breast cancer based on fine needle biopsy microscopic images, *Comput. Biol. Med.* 43 (10) (2013) 1563–1572.
- [52] A. Vahadane, A. Sethi, Towards Generalized Nuclear Segmentation in Histological Images, 2013, pp. 1–4.
- [53] M. Aswathy, M. Jagannath, Performance analysis of segmentation algorithms for the detection of breast cancer, *Procedia Comput. Sci.* 167 (2020) 666–676.
- [54] A. Mouelhi, H. Rmili, J.B. Ali, M. Sayadi, R. Doghri, K. Mrad, Fast unsupervised nuclear segmentation and classification scheme for automatic allred cancer scoring in immunohistochemical breast tissue images, *Comput. Methods Progr. Biomed.* 165 (2018) 37–51.
- [55] M. López, N. Posada, J. Gadelha, F. Morgado, Deformable models as a tool for biometric and histopathological applications, *Microsc. Microanal.* 19 (S4) (2013) 75–76.
- [56] E.A. Mohammed, M.M. Mohamed, C. Naugler, B.H. Far, Chronic Lymphocytic Leukemia Cell Segmentation from Microscopic Blood Images Using Watershed Algorithm and Optimal Thresholding, 2013, pp. 1–5.
- [57] B.-B. Kamel, J. Prescott, G. Lozanski, M.N. Gurcan, Segmentation of follicular regions on h&e slides using a matching filter and active contour model 7624, 2010, 762436.
- [58] M.M. Dundar, S. Badve, G. Bilgin, V. Raykar, R. Jain, O. Sertel, M.N. Gurcan, Computerized classification of intraductal breast lesions using histopathological images, *IEEE (Inst. Electr. Electron. Eng.) Trans. Biomed. Eng.* 58 (7) (2011) 1977–1984.
- [59] E. Reinhard, M. Adhikmin, B. Gooch, P. Shirley, Color transfer between images, *IEEE Comput. Graph. Appl.* 21 (5) (2001) 34–41.
- [60] A. Rabinovich, S. Agarwal, C. Laris, J. Price, S. Belongie, Unsupervised color decomposition of histologically stained tissue samples, *Adv. Neural Inf. Process. Syst.* 16 (2003) 667–674.
- [61] M. Macenko, M. Niethammer, J.S. Marron, D. Borland, J.T. Woosley, X. Guan, C. Schmitt, N.E. Thomas, A Method for Normalizing Histology Slides for Quantitative Analysis, 2009, pp. 1107–1110.
- [62] A.M. Khan, N. Rajpoot, D. Treanor, D. Magee, A nonlinear mapping approach to stain normalization in digital histopathology images using image-specific color deconvolution, *IEEE (Inst. Electr. Electron. Eng.) Trans. Biomed. Eng.* 61 (6) (2014) 1729–1738.
- [63] R.A. Hoffman, S. Kothari, M.D. Wang, Comparison of Normalization Algorithms for Cross-Batch Color Segmentation of Histopathological Images, 2014, pp. 194–197.
- [64] A. Vahadane, T. Peng, A. Sethi, S. Albarqouni, L. Wang, M. Baust, K. Steiger, A. M. Schlitter, I. Esposito, N. Navab, Structure-preserving color normalization and sparse stain separation for histological images, *IEEE Trans. Med. Imag.* 35 (8) (2016) 1962–1971.
- [65] T.A.A. Tosta, P.R. de Faria, J.P.S. Servato, L.A. Neves, G.F. Roberto, A.S. Martins, M.Z. do Nascimento, Unsupervised method for normalization of hematoxylin-eosin stain in histological images, *Comput. Med. Imag. Graph.* 77 (2019), 101646.
- [66] Y. Zheng, Z. Jiang, H. Zhang, F. Xie, J. Shi, C. Xue, Adaptive color deconvolution for histological wsi normalization, *Comput. Methods Progr. Biomed.* 170 (2019) 107–120.
- [67] M. Salvi, N. Michielli, F. Molinari, Stain color adaptive normalization (scan) algorithm: separation and standardization of histological stains in digital pathology, *Comput. Methods Progr. Biomed.* 193 (2020), 105506.
- [68] S. Vijh, M. Saraswat, S. Kumar, A new complete color normalization method for h&e stained histopathological images, *Appl. Intell.* 51 (11) (2021) 7735–7748.
- [69] M. Salvi, F. Molinari, Multi-tissue and multi-scale approach for nuclei segmentation in h&e stained images, *Biomed. Eng. Online* 17 (1) (2018) 1–13.
- [70] M.N. Gurcan, T. Pan, H. Shimada, J. Saltz, Image Analysis for Neuroblastoma Classification: Segmentation of Cell Nuclei, 2006, pp. 4844–4847.
- [71] S. Petushi, F.U. Garcia, M.M. Haber, C. Katsinis, A. Tozeren, Large-scale computations on histology images reveal grade-differentiating parameters for breast cancer, *BMC Med. Imag.* 6 (1) (2006) 1–11.
- [72] C. Lu, M. Mandal, Toward automatic mitotic cell detection and segmentation in multispectral histopathological images, *IEEE J. Biomed. Health Inf.* 18 (2) (2013) 594–605.
- [73] P. Filipczuk, M. Kowal, A. Obuchowicz, Breast Fibroadenoma Automatic Detection Using K-Means Based Hybrid Segmentation Method, 2012.
- [74] L. Liu, D. Zhao, F. Yu, A.A. Heidari, J. Ru, H. Chen, M. Mafarja, H. Turabieh, Z. Pan, Performance optimization of differential evolution with slime mould algorithm for multilevel breast cancer image segmentation, *Comput. Biol. Med.* 138 (2021), 104910.
- [75] J. Malek, A. Sebri, S. Mabrouk, K. Torki, R. Tourki, Automated breast cancer diagnosis based on gvf-snake segmentation, wavelet features extraction and fuzzy classification, *J. Signal Process Syst.* 55 (1) (2009) 49–66.
- [76] L. Yang, O. Tuzel, P. Meer, D.J. Foran, Automatic Image Analysis of Histopathology Specimens Using Concave Vertex Graph, 2008, pp. 833–841.
- [77] J. Xu, A. Janowczyk, S. Chandran, A. Madabhushi, A high-throughput active contour scheme for segmentation of histopathological imagery, *Med. Image Anal.* 15 (6) (2011) 851–862.
- [78] H. Fatakdawala, J. Xu, A. Basavanhally, G. Bhanot, S. Ganesan, M. Feldman, J. E. Tomaszewski, A. Madabhushi, Expectation–maximization-driven geodesic active contour with overlap resolution (emagacor): application to lymphocyte segmentation on breast cancer histopathology, *IEEE (Inst. Electr. Electron. Eng.) Trans. Biomed. Eng.* 57 (7) (2010) 1676–1689.
- [79] S. Ali, A. Madabhushi, An integrated region-, boundary-, shape-based active contour for multiple object overlap resolution in histological imagery, *IEEE Trans. Med. Imag.* 31 (7) (2012) 1448–1460.
- [80] A. Mouelhi, M. Sayadi, F. Fnaiech, K. Mrad, K.B. Romdhane, Automatic image segmentation of nuclear stained breast tissue sections using color active contour model and an improved watershed method, *Biomed. Signal Process Control* 8 (5) (2013) 421–436.
- [81] J.A.A. Jothi, V.M.A. Rajam, Effective segmentation of orphan annie-eye nuclei from papillary thyroid carcinoma histopathology images using a probabilistic model and region-based active contour, *Biomed. Signal Process Control* 30 (2016) 149–161.
- [82] O. Sertel, J. Kong, G. Lozanski, U. Catalyurek, J.H. Saltz, M.N. Gurcan, Computerized microscopic image analysis of follicular lymphoma 6915 (2008) 974–984.
- [83] O. Sertel, J. Kong, G. Lozanski, A. Shana'ah, U. Catalyurek, J. Saltz, M. Gurcan, Texture Classification Using Nonlinear Color Quantization: Application to Histopathological Image Analysis, 2008, pp. 597–600.
- [84] K. Dimitropoulos, P. Barmptouli, T. Koletsas, I. Kostopoulos, N. Grammalidis, Automated detection and classification of nuclei in pax5 and h&e-stained tissue sections of follicular lymphoma, *Signal Image Video Process.* 11 (1) (2017) 145–153.
- [85] O. Sertel, U.V. Catalyurek, G. Lozanski, A. Shanaah, M.N. Gurcan, An Image Analysis Approach for Detecting Malignant Cells in Digitized H&E-Stained Histology Images of Follicular Lymphoma, 2010, pp. 273–276.
- [86] C. Lu, M. Mahmood, N. Jha, M. Mandal, Automated segmentation of the melanocytes in skin histopathological images, *IEEE J. Biomed. Health Inf.* 17 (2) (2013) 284–296.
- [87] P. Filipczuk, M. Kowal, A. Obuchowicz, Fuzzy Clustering and Adaptive Thresholding Based Segmentation Method for Breast Cancer Diagnosis, 2011, pp. 613–622.
- [88] P.-W. Huang, Y.-H. Lai, Effective segmentation and classification for hcc biopsy images, *Pattern Recogn.* 43 (4) (2010) 1550–1563.
- [89] Y.M. George, B.M. Bagoury, H.H. Zayed, M.I. Roushdy, Automated cell nuclei segmentation for breast fine needle aspiration cytology, *Signal Process.* 93 (10) (2013) 2804–2816.
- [90] C. Jung, C. Kim, Segmenting clustered nuclei using h-minima transform-based marker extraction and contour parameterization, *IEEE Trans. Biomed. Eng.* 57 (10) (2010) 2600–2604.
- [91] M. Veta, P.J. Van Diest, R. Kornegoor, A. Huisman, M.A. Viergever, J.P. Pluim, Automatic nuclei segmentation in h&e stained breast cancer histopathology images, *PLoS One* 8 (7) (2013), e70221.
- [92] P.J. Schüffler, D. Schapiro, C. Giesen, H.A. Wang, B. Bodenmiller, J.M. Buhmann, Automatic single cell segmentation on highly multiplexed tissue images, *Cytometry* 87 (10) (2015) 936–942.
- [93] O. Schmitt, M. Hasse, Radial symmetries based decomposition of cell clusters in binary and gray level images, *Pattern Recogn.* 41 (6) (2008) 1905–1923.
- [94] J. Cheng, J.C. Rajapakse, et al., Segmentation of clustered nuclei with shape markers and marking function, *IEEE (Inst. Electr. Electron. Eng.) Trans. Biomed. Eng.* 56 (3) (2008) 741–748.
- [95] H. Wang, A.C. Roa, A.N. Basavanhally, H.L. Gilmore, N. Shih, M. Feldman, J. Tomaszewski, F. Gonzalez, A. Madabhushi, Mitosis detection in breast cancer pathology images by combining handcrafted and convolutional neural network features, *J. Med. Imag.* 1 (3) (2014), 034003.
- [96] H. Chen, X. Qi, L. Yu, Q. Dou, J. Qin, P.-A. Heng, Dcan: deep contour-aware networks for object instance segmentation from histology images, *Med. Image Anal.* 36 (2017) 135–146.
- [97] M.Z. Alom, C. Yakopcic, T.M. Taha, V.K. Asari, Nuclei Segmentation with Recurrent Residual Convolutional Neural Networks Based U-Net (R2u-net), 2018, pp. 228–233.
- [98] S. Özürk, B. Akdemir, Cell-type based semantic segmentation of histopathological images using deep convolutional neural networks, *Int. J. Imag. Syst. Technol.* 29 (3) (2019) 234–246.
- [99] E. Shelhamer, J. Long, T. Darrell, Fully convolutional networks for semantic segmentation, *IEEE Trans. Pattern Anal. Mach. Intell.* 39 (4) (2017) 640–651.
- [100] Y. Cui, G. Zhang, Z. Liu, Z. Xiong, J. Hu, A deep learning algorithm for one-step contour aware nuclei segmentation of histopathology images, *Med. Biol. Eng. Comput.* 57 (9) (2019) 2027–2043.
- [101] Q. Kang, Q. Lao, T. Fevens, Nuclei Segmentation in Histopathological Images Using Two-Stage Learning, 2019, pp. 703–711.
- [102] B.M. Priego-Torres, D. Sanchez-Morillo, M.A. Fernandez-Granero, M. Garcia-Rojo, Automatic segmentation of whole-slide h&e stained breast histopathology images using a deep convolutional neural network architecture, *Expert Syst. Appl.* 151 (2020), 113387.
- [103] D. Kucharski, P. Kleczek, J. Jaworek-Korjakowska, G. Dyduch, M. Gorgon, Semi-supervised nests of melanocytes segmentation method using convolutional autoencoders, *Sensors* 20 (6) (2020) 1546.

- [104] M. Salvi, M. Bosco, L. Molinaro, A. Gambella, M. Papotti, U.R. Acharya, F. Molinari, A hybrid deep learning approach for gland segmentation in prostate histopathological images, *Artif. Intell. Med.* 115 (2021) 102076.
- [105] X. Zhang, X. Zhu, K. Tang, Y. Zhao, Z. Lu, Q. Feng, Ddtnet, A Dense Dual-Task Network for Tumor-Infiltrating Lymphocyte Detection and Segmentation in Histopathological Images of Breast Cancer, *Medical Image Analysis*, 2022, 102415.
- [106] I. Kiran, B. Raza, A. Ijaz, M.A. Khan, Denserest-unet: segmentation of overlapped/clustered nuclei from multi organ histopathology images, *Comput. Biol. Med.* (2022), 105267.
- [107] A. Tashk, M.S. Helfroush, H. Danyali, M. Akbarzadeh-Jahromi, Automatic detection of breast cancer mitotic cells based on the combination of textural, statistical and innovative mathematical features, *Appl. Math. Model.* 39 (20) (2015) 6165–6182.
- [108] P. Wang, S. Xu, Y. Li, L. Wang, Q. Song, Feature-based analysis of cell nuclei structure for classification of histopathological images, *Digit. Signal Process.* 78 (2018) 152–162.
- [109] K. Fukuma, V.S. Prasath, H. Kawanaka, B.J. Aronow, H. Takase, A study on nuclei segmentation, feature extraction and disease stage classification for human brain histopathological images, *Procedia Comput. Sci.* 96 (2016) 1202–1210.
- [110] O. Sertel, J. Kong, U.V. Catalyurek, G. Lozanski, J.H. Saltz, M.N. Gurcan, Histopathological image analysis using model-based intermediate representations and color texture: follicular lymphoma grading, *J. Signal Process Syst.* 55 (1) (2009) 169–183.
- [111] H. Kong, M. Gurcan, K. Belkacem-Boussaid, Partitioning histopathological images: an integrated framework for supervised color-texture segmentation and cell splitting, *IEEE Trans. Med. Imag.* 30 (9) (2011) 1661–1677.
- [112] B.E. Bejnordi, N. Timofeeva, I. Otte-Höller, N. Karssemeijer, J.A. van der Laak, Quantitative Analysis of Stain Variability in Histology Slides and an Algorithm for Standardization 9041, 2014, 904108.
- [113] R. Rashmi, K. Prasad, C.B.K. Udupa, V. Shwetha, A comparative evaluation of texture features for semantic segmentation of breast histopathological images, *IEEE Access* 8 (2020) 64331–64346.
- [114] S. Chen, J. Yu, R. Ruan, Y. Li, Y. Tao, Q. Shen, Z. Cui, C. Shen, H. Wang, J. Jin, et al., “Pink pattern” visualized in magnifying endoscopy with narrow-band imaging is a novel feature of early differentiated gastric cancer: a bridge between endoscopic images and histopathological changes, *Front. Med.* 8 (2021).
- [115] N. Kumar, M. Sharma, V.P. Singh, C. Madan, S. Mehandia, An empirical study of handcrafted and dense feature extraction techniques for lung and colon cancer classification from histopathological images, *Biomed. Signal Process Control* 75 (2022), 103596.
- [116] A. Albayrak, G. Bilgin, Breast Cancer Mitosis Detection in Histopathological Images with Spatial Feature Extraction 9067, 2013, 90670L.
- [117] M.M.R. Krishnan, V. Venkatraghavan, U.R. Acharya, M. Pal, R.R. Paul, L.C. Min, A.K. Ray, J. Chatterjee, C. Chakraborty, Automated oral cancer identification using histopathological images: a hybrid feature extraction paradigm, *Micron* 43 (2–3) (2012) 352–364.
- [118] D.O.T. Bruno, M.Z. Do Nascimento, R.P. Ramos, V.R. Batista, L.A. Neves, A. S. Martins, Lbp operators on curvelet coefficients as an algorithm to describe texture in breast cancer tissues, *Expert Syst. Appl.* 55 (2016) 329–340.
- [119] H.A. Phouladhy, M. Zhou, D.B. Goldgof, L.O. Hall, P.R. Mouton, Automatic Quantification and Classification of Cervical Cancer via Adaptive Nucleus Shape Modeling, 2016, pp. 2658–2662.
- [120] R. Peyret, A. Bouridane, F. Khelifi, M.A. Tahir, S. Al-Maadeed, Automatic classification of colorectal and prostatic histologic tumor images using multiscale multispectral local binary pattern texture features and stacked generalization, *Neurocomputing* 275 (2018) 83–93.
- [121] Ş. Öztürk, B. Akdemir, Application of feature extraction and classification methods for histopathological image using glcm, lbp, lbgclcm, grlcm and sfta, *Procedia Comput. Sci.* 132 (2018) 40–46.
- [122] Y. Zheng, Z. Jiang, F. Xie, H. Zhang, Y. Ma, H. Shi, Y. Zhao, Feature extraction from histopathological images based on nucleus-guided convolutional neural network for breast lesion classification, *Pattern Recogn.* 71 (2017) 14–25.
- [123] A. Yonekura, H. Kawanaka, V. Prasath, B.J. Aronow, H. Takase, Automatic disease stage classification of glioblastoma multiforme histopathological images using deep convolutional neural network, *Biomed. Eng. Lett.* 8 (3) (2018) 321–327.
- [124] R. Mehra, et al., Breast cancer histology images classification: training from scratch or transfer learning? *ICT Express* 4 (4) (2018) 247–254.
- [125] J. Xie, R. Liu, J. Luttrell IV, C. Zhang, Deep learning based analysis of histopathological images of breast cancer, *Front. Genet.* 10 (2019) 80.
- [126] D.M. Vo, N. Nguyen, S. Lee, Classification of breast cancer histology images using incremental boosting convolution networks, *Inf. Sci.* 482 (2019) 123–138.
- [127] K. George, S. Faziludeen, P. Sankaran, J.K. Paul, Deep Learned Nucleus Features for Breast Cancer Histopathological Image Analysis Based on Belief Theoretical Classifier Fusion, 2019, pp. 344–349.
- [128] V. Kate, P. Shukla, A 3 tier cnn model with deep discriminative feature extraction for discovering malignant growth in multi-scale histopathology images, *Inform. Med. Unlocked* 24 (2021), 100616.
- [129] R. Rashmi, K. Prasad, C.B.K. Udupa, Bchisto-net: breast histopathological image classification by global and local feature aggregation, *Artif. Intell. Med.* 121 (2021), 102191.
- [130] S. Sharma, S. Kumar, The exception model: a potential feature extractor in breast cancer histology images classification, *ICT Express* 8 (1) (2022) 101–108.
- [131] G. Huang, Z. Liu, L. Van Der Maaten, K.Q. Weinberger, Densely Connected Convolutional Networks, 2017, pp. 4700–4708.
- [132] T.Y. Rahman, L.B. Mahanta, A.K. Das, J.D. Sarma, Automated oral squamous cell carcinoma identification using shape, texture and color features of whole image strips, *Tissue Cell* 63 (2020) 101322.
- [133] M.E. Bagdigen, G. Bilgin, Detection and Grading of Breast Cancer via Spatial Features in Histopathological Images, 2019, pp. 1–4.
- [134] S.A. Korkmaz, Recognition of the gastric molecular image based on decision tree and discriminant analysis classifiers by using discrete fourier transform and features, *Appl. Artif. Intell.* 32 (7–8) (2018) 629–643.
- [135] T.Y. Rahman, L.B. Mahanta, H. Choudhury, A.K. Das, J.D. Sarma, Study of morphological and textural features for classification of oral squamous cell carcinoma by traditional machine learning techniques, *Cancer Rep.* 3 (6) (2020), e1293.
- [136] M. Kuse, T. Sharma, S. Gupta, A classification scheme for lymphocyte segmentation in h&e stained histology images, 2010, pp. 235–243.
- [137] M.M.R. Krishnan, C. Chakraborty, R.R. Paul, A.K. Ray, Hybrid segmentation, characterization and classification of basal cell nuclei from histopathological images of normal oral mucosa and oral submucous fibrosis, *Expert Syst. Appl.* 39 (1) (2012) 1062–1077.
- [138] Y. Xu, L. Jiao, S. Wang, J. Wei, Y. Fan, M. Lai, E. Chang, Multi-label classification for colon cancer using histopathological images, *Microsc. Res. Tech.* 76 (12) (2013) 1266–1277.
- [139] O.S. Al-Kadi, A multiresolution clinical decision support system based on fractal model design for classification of histological brain tumours, *Comput. Med. Imag. Graph.* 41 (2015) 67–79.
- [140] A. Masood, A. Al-Jumaily, Differential Evolution Based Advised Svm for Histopathological Image Analysis for Skin Cancer Detection, 2015, pp. 781–784.
- [141] S.I. Niwas, P. Palanisamy, K. Sujathan, E. Bengtsson, Analysis of nuclei textures of fine needle aspirated cytology images for breast cancer diagnosis using complex daubechies wavelets, *Signal Process.* 93 (10) (2013) 2828–2837.
- [142] J. Han, H. Chang, L. Loss, K. Zhang, F.L. Baehner, J.W. Gray, P. Spellman, B. Parvin, Comparison of Sparse Coding and Kernel Methods for Histopathological Classification of Glioblastoma Multiforme, 2011, pp. 711–714.
- [143] N.N. Shirale, Sparse Representation Based Class Level Dictionary Learning Approach for Histopathology Image Classification, 2018, pp. 1–5.
- [144] X. Li, H. Tang, D. Zhang, T. Liu, L. Mao, T. Chen, Histopathological image classification through discriminative feature learning and mutual information-based multi-channel joint sparse representation, *J. Vis. Commun. Image Represent.* 70 (2020), 102799.
- [145] P. Stanitsas, A. Cherian, X. Li, A. Truskovsky, V. Morellas, N. Papanikopoulos, Evaluation of Feature Descriptors for Cancerous Tissue Recognition, 2016, pp. 1490–1495.
- [146] Y. Zheng, Z. Jiang, F. Xie, H. Zhang, Y. Ma, H. Shi, Y. Zhao, Feature extraction from histopathological images based on nucleus-guided convolutional neural network for breast lesion classification, *Pattern Recogn.* 71 (2017) 14–25.
- [147] Z. Han, B. Wei, Y. Zheng, Y. Yin, K. Li, S. Li, Breast cancer multi-classification from histopathological images with structured deep learning model, *Sci. Rep.* 7 (1) (2017) 1–10.
- [148] B.E. Bejnordi, J. Lin, B. Glass, M. Mullooly, G.L. Gierach, M.E. Sherman, N. Karssemeijer, J. Van Der Laak, A.H. Beck, Deep Learning-Based Assessment of Tumor-Associated Stroma for Diagnosing Breast Cancer in Histopathology Images, 2017, pp. 929–932.
- [149] Z. Gandomkar, P.C. Brennan, C. Mello-Thoms, Mudern, Multi-category classification of breast histopathological image using deep residual networks, *Artif. Intell. Med.* 88 (2018) 14–24.
- [150] Ş. Öztürk, B. Akdemir, Hic-net: a deep convolutional neural network model for classification of histopathological breast images, *Comput. Electr. Eng.* 76 (2019) 299–310.
- [151] H. Saito, T. Aoki, K. Aoyama, Y. Kato, A. Tsuboi, A. Yamada, M. Fujishiro, S. Oka, S. Ishihara, T. Matsuda, et al., Automatic detection and classification of protruding lesions in wireless capsule endoscopy images based on a deep convolutional neural network, *Gastrointest. Endosc.* 92 (1) (2020) 144–151.
- [152] S. Panigrahi, J. Das, T. Swarnkar, Capsule Network Based Analysis of Histopathological Images of Oral Squamous Cell Carcinoma, *Journal of King Saud University-Computer and Information Sciences*, 2020.
- [153] A. Kumar, S.K. Singh, S. Saxena, K. Lakshmanan, A.K. Sangaiyah, H. Chauhan, S. Shrivastava, R.K. Singh, Deep feature learning for histopathological image classification of canine mammary tumors and human breast cancer, *Inf. Sci.* 508 (2020) 405–421.
- [154] K.C. Burçak, Ö.K. Baykan, H. Uğuz, A new deep convolutional neural network model for classifying breast cancer histopathological images and the hyperparameter optimisation of the proposed model, *J. Supercomput.* 77 (1) (2021) 973–989.
- [155] V. Gupta, M. Vasudev, A. Doegar, N. Sambyal, Breast cancer detection from histopathology images using modified residual neural networks, *Biocybern. Biomed. Eng.* 41 (4) (2021) 1272–1287.
- [156] P. Wang, J. Wang, Y. Li, P. Li, L. Li, M. Jiang, Automatic classification of breast cancer histopathological images based on deep feature fusion and enhanced routing, *Biomed. Signal Process Control* 65 (2021), 102341.
- [157] L. Su, Y. Liu, M. Wang, A. Li, Semi-hic: a novel semi-supervised deep learning method for histopathological image classification, *Comput. Biol. Med.* 137 (2021), 104788.
- [158] R. Yan, F. Ren, Z. Wang, L. Wang, T. Zhang, Y. Liu, X. Rao, C. Zheng, F. Zhang, Breast cancer histopathological image classification using a hybrid deep neural network, *Methods* 173 (2020) 52–60.
- [159] A.A. Joseph, M. Abdulla, S.B. Junaidi, H.H. Ibrahim, H. Chiroma, Improved multi-classification of breast cancer histopathological images using handcrafted

- features and deep neural network (dense layer), *Intell. Syst. Appl.* 14 (2022), 200066.
- [160] S. Chattopadhyay, A. Dey, P.K. Singh, R. Sarkar, Drda-net: dense residual dual-shuffle attention network for breast cancer classification using histopathological images, *Comput. Biol. Med.* (2022), 105437.
- [161] C. Wang, W. Gong, J. Cheng, Y. Qian, Dblcnn: dependency-based lightweight convolutional neural network for multi-classification of breast histopathology images, *Biomed. Signal Process Control* 73 (2022), 103451.
- [162] A. Jaiswal, W. AbdAlmageed, Y. Wu, P. Natarajan, Capsulegan: Generative Adversarial Capsule Network, 2018, 0–0.
- [163] R. Man, P. Yang, B. Xu, Classification of breast cancer histopathological images using discriminative patches screened by generative adversarial networks, *IEEE Access* 8 (2020) 155362–155377.
- [164] D. Wang, Z. Chen, H. Zhao, Prototype transfer generative adversarial network for unsupervised breast cancer histology image classification, *Biomed. Signal Process Control* 68 (2021), 102713.
- [165] Y. Xue, J. Ye, Q. Zhou, L.R. Long, S. Antani, Z. Xue, C. Cornwell, R. Zaino, K. C. Cheng, X. Huang, Selective synthetic augmentation with histogan for improved histopathology image classification, *Med. Image Anal.* 67 (2021), 101816.
- [166] W. Li, J. Li, J. Polson, Z. Wang, W. Speier, C. Arnold, High resolution histopathology image generation and segmentation through adversarial training, *Med. Image Anal.* 75 (2022) 102251.
- [167] P. Alirezazadeh, B. Hejriati, A. Monsef-Esfahani, A. Fathi, Representation learning-based unsupervised domain adaptation for classification of breast cancer histopathology images, *Biocybern. Biomed. Eng.* 38 (3) (2018) 671–683.
- [168] X. Yu, H. Zheng, C. Liu, Y. Huang, X. Ding, Classify epithelium-stroma in histopathological images based on deep transferable network, *J. Microsc.* 271 (2) (2018) 164–173.
- [169] G. Figueira, Y. Wang, L. Sun, H. Zhou, Q. Zhang, Adversarial-based Domain Adaptation Networks for Unsupervised Tumour Detection in Histopathology, 2020, pp. 1284–1288.
- [170] P. Wang, P. Li, Y. Li, J. Xu, M. Jiang, Classification of histopathological whole slide images based on multiple weighted semi-supervised domain adaptation, *Biomed. Signal Process Control* 73 (2022), 103400.
- [171] J. Shi, J. Wu, Y. Li, Q. Zhang, S. Ying, Histopathological image classification with color pattern random binary hashing-based pcanet and matrix-form classifier, *IEEE J. Biomed. Health Inf.* 21 (5) (2016) 1327–1337.
- [172] R. Mukkamala, P.S. Neeraja, S. Pamidi, T. Babu, T. Singh, Deep Pcanet Framework for the Binary Categorization of Breast Histopathology Images, 2018, pp. 105–110.
- [173] J. Shi, X. Zheng, J. Wu, B. Gong, Q. Zhang, S. Ying, Quaternion grassmann average network for learning representation of histopathological image, *Pattern Recogn.* 89 (2019) 67–76.
- [174] J. Zhang, W. Cui, X. Guo, B. Wang, Z. Wang, Classification of digital pathological images of non-hodgkin's lymphoma subtypes based on the fusion of transfer learning and principal component analysis, *Med. Phys.* 47 (9) (2020) 4241–4253.
- [175] W. Samek, A. Binder, G. Montavon, S. Lapuschkin, K.-R. Müller, Evaluating the visualization of what a deep neural network has learned, *IEEE Transact. Neural Networks Learn. Syst.* 28 (11) (2016) 2660–2673.